Climate evolution in the Adriatic Sea across the last deglaciation: A multiproxy approach combining biomarkers and calcareous plankton

Pietro Bazzicalupo, Marie-Alexandrine Sicre, Helena Checa, Patrizia Maiorano, Giulia Margaritelli, Vincent Klein, Leopoldo David Pena, Isabel Cacho, Jaime Frigola, Sergio Bonomo, et al.

Palaeogeography, Palaeoclimatology, Palaeoecology

Climate evolution in the Adriatic Sea across the last deglaciation: a multiproxy approach combining biomarkers and calcareous plankton

--Manuscript Draft--

Manuscript Number:	PALAEO-D-22-00309
Article Type:	Research Paper
Keywords:	deglaciation; Heinrich Stadial 1; Adriatic Sea; terrestrial and marine biomarkers; calcareous plankton; Climate forcing
Corresponding Author:	Pietro Bazzicalupo, Ph.D. University of Milano–Bicocca: Universita degli Studi di Milano-Bicocca Milano, ITALY
First Author:	Pietro Bazzicalupo, Ph.D.
Order of Authors:	Pietro Bazzicalupo, Ph.D.
	Marie-Alexandrine Sicre, PhD
	Helena Checa
	Patrizia Maiorano, PhD
	Giulia Margaritelli, PhD
	Vincent Klein, PhD
	David Leopoldo Pena, PhD
	Isabel Cacho, PhD
	Jaime Frigola, PhD
	Sergio Bonomo, PhD
	Antonio Cascella, PhD
	Fabrizio Lirer, PhD
Manuscript Region of Origin:	Europe
Abstract:	A multiproxy study combining calcareous plankton assemblages (coccolithophore and planktonic foraminifera), and terrestrial (n-alkanes) and marine (alkenones) biomarkers was carried out in a sediment core (ND14Q-AR2) from the South Adriatic Sea. The focus of the study is to investigate millennial-to-centennial scale climate variability in the Eastern Mediterranean during the last deglaciation, between 20 and 11 ka BP. The high-resolution reconstruction allows for the characterization of the impact of the Heinrich Stadial 1 (HS1, here identified between 17.1 and 14.9 ka BP) at a centennial/multi-decadal time scale resolution. Based on terrestrial proxies, the HS1 interval has a two-fold partition: HS1a (17.1-15.9 ka BP), characterized by decreasing temperatures and relative high humidity, and HS1b (15.9-14.9 ka BP), characterized by the coldest temperatures and drier conditions on land. Terrestrial proxies suggest changes in moisture availability on land and ice melting delivery from the Alps during HS1. This period is followed by the Bølling-Allerød record (B-A, 14.9-12.3 ka BP) indicating ameliorated climate conditions and distinct local hydrological signals, related to global melt event similar to the Melt Water Pulse-1A. Finally, the comparison of our results with other Northern Hemisphere climatic records shows a good correspondence between the temperature variations in the South Adriatic Sea and the Greenland ice core oxygen isotope record, highlighting the climatic response of the South Adriatic to global climate variations. Comparison with other Mediterranean paleoclimatic records suggests a two-steps reorganization of the ocean/atmospheric circulation during the HS1 in the mid- and low-latitudes during the HS1 interval, but also a connection with the tropical Northern Hemisphere climate.
Suggested Reviewers:	Barbara Balestra, PhD Lab Director, American University balestra@american.edu

	Expertise on coccolithophore ecology
	Antonio Caruso, PhD Full Professor, University of Palermo: Universita degli Studi di Palermo antonio.caruso@unipa.it Expertise on planktonic foraminifera
	Blanca Ausin, PhD Assistant Professor, Universidad de Salamanca ausin@usal.es Expertise on coccolithophore and alkenones
	Francisco Javier Sierro, PhD Full Professor, Universidad de Salamanca sierro@usal.es Expertise in paleoceanography
	Teresa Rodrigues, PhD IPMA: Instituto Portugues do Mar e da Atmosfera teresa.rodrigues@ipma.pt Expertise on biomarkers

Highlights:

- Planktonic assemblages and marine/terrestrial biomarker comparison.
- Late deglaciation, Heinrich Stadial 1 and Bølling-Allerød in the South Adriatic Sea.
- Two-step division of Heinrich Stadial 1, following changes in humidity on land.
- Melting water during the deglaciation inferred by planktonic assemblage proxies.
- Heinrich Stadial 1 partition well correlated with other paleoclimatic records.

Climate evolution in the Adriatic Sea across the last deglaciation: a multiproxy approach combining biomarkers and calcareous plankton

Bazzicalupo Pietro[1,4], Sicre Marie-Alexandrine[2], Checa Helena[3,6], Maiorano Patrizia[4], Margaritelli Giulia[5], Klein Vincent[2], Pena Leopoldo David[6], Cacho Isabel[6], Frigola Jaime[6], Bonomo Sergio[7], Cascella Antonio[8], Lirer Fabrizio[9]

[1]Dipartimento di Scienze della Terra e Ambientali, Università degli Studi di Milano-Bicocca, P.zza della Scienza 4, 20126, Milan, Italy.
[2]LOCEAN, CNRS, SorbonneUniversité, Campus Pierre et Marie-Curie, Paris, France.
[3]Dipartimento di Fisica e Geologia, Università di Perugia, Via Alessandro Pascoli, 06123, Perugia, Italy.
[4]Dipartimento di Scienze della Terra e Geoambientali, Università degli Studi di Bari Aldo Moro, via E. Orabona 4, 70125, Bari, Italy.
[5] Istituto di Ricerca per la Protezione Idrogeologica (IRPI-CNR), Consiglio Nazionale delle Ricerche, via Madonna Alta 126, 06128, Perugia, Italy.
[6]GRC Geociències Marines, Dept. de Dinàmica de la Terra i de l'Oceà, FacultatdeCiències de la Terra, Universitat de Barcelona. C/ Martí i Franqués s/n 08028, Barcelona, Spain.
[7]Institute of Environmental Geology and Geoengineering, National Research Council (IGAG-CNR), Via Salaria km 29,300 – 00015, Monterotondo (RM), Italy.
[8]Istituto Nazionale di Geofisica e Vulcanologia, Via della Faggiola 32, 52126 Pisa, Italy.
[9]Dipartimento di Scienze della Terra, Sapienza Università di Roma, P. Aldo Moro 5, 00185 Roma, Italy.

Keywords

Deglaciation, Heinrich Stadial 1, Adriatic Sea, terrestrial and marine biomarkers, calcareous plankton, climate forcing.

Abstract

A multiproxy study combining calcareous plankton assemblages (coccolithophore and planktonic foraminifera), and terrestrial (n-alkanes) and marine (alkenones) biomarkers was carried out in a sediment core (ND14Q-AR2) from the South Adriatic Sea. The focus of the study is to investigate millennial-to-centennial scale climate variability in the Eastern Mediterranean during the last deglaciation, between 20 and 11 ka BP. The high-resolution reconstruction allows for the characterization of the impact of the Heinrich Stadial 1 (HS1, here identified between 17.1 and 14.9 ka BP) at a centennial/multi-decadal time scale resolution. Based on terrestrial proxies, the HS1 interval has a two-fold partition: HS1a (17.1-15.9 ka BP), characterized by decreasing temperatures and relative high humidity, and HS1b (15.9-14.9 ka BP), characterized by the coldest temperatures and drier conditions on land. Terrestrial proxies suggest changes in moisture availability on land and ice melting delivery from the Alps during HS1. This period is followed by the Bølling-Allerød record (B-A, 14.9-12.3 ka BP) indicating ameliorated climate conditions and distinct local hydrological signals, related to global melt event similar to the Melt Water Pulse-1A. Finally, the comparison of our results with other Northern Hemisphere climatic records shows a good correspondence between the temperature variations in the South Adriatic Sea and the Greenland ice core oxygen isotope record, highlighting the climatic response of the South Adriatic to global climate variations. Comparison with other Mediterranean paleoclimatic records suggests a two-steps reorganization of the ocean/atmospheric circulation during the HS1 in the mid- and low-latitudes during the HS1 interval, but also a connection with the tropical Northern Hemisphere climate.

1. Introduction

The last deglaciation was punctuated by a series of large amplitude oscillations that left a distinct imprint in the North Atlantic and Greenland records (Bond et al., 1992; Broecker et al., 1992; Dansgaard et al., 1993; Bard et al., 2000; Rasmussen et al., 2006; Stanford et al., 2011; Clark et al., 2012; Schwab et al., 2012; Toucanne et al., 2015; Repschläger et al., 2015; Hodell et al., 2017). Across this transition, the most severe climatic period known as the Heinrich Stadial 1 (HS1) is well documented in the western Mediterranean (e.g. Martrat et al., 2004, 2014; Sierro et al., 2005; Combourieu Nebout et al., 2009; Rogerson et al., 2010; Ausín et al., 2015; Naughton et al., 2016; Bazzicalupo et al., 2018). Cold and fresher water inflow from iceberg melting through Strait of Gibraltar most likely caused significant modification of the water column (Cacho et al., 1999; Pérez-Folgado et al., 2003; Colmenero-Hidalgo et al., 2004; Martrat et al., 2004, 2014; Sierro et al., 2005; Jiménez-Amat and Zahn, 2015; Toucanne et al., 2015) and notable changes on land in southern Europe (Allen et al., 1999; Sanchez Goñi et al., 2002; Combourieu Nebout et al., 2009; Naughton et al., 2016). Several records of HS1 (ca. 17.5–14.5 ka BP) in the western Mediterranean pointed out the complexity of this interval involving changes in the atmospheric circulation and inflow of cold Atlantic waters (Moreno et al., 2005; Fletcher and Sánchez Goñi, 2008; Frigola et al., 2008; Melki et al., 2009; Rodrigo-Gámiz et al., 2011; Martinez-Ruiz et al., 2015; Bazzicalupo et al., 2018). Other studies in the central and eastern Mediterranean revealed that the impact of HS1 was not confined to the western Mediterranean and Atlantic region and that the eastern basin experienced marked cold and arid climate conditions during this period (Kwiecien et al., 2009; Kotthoff et al., 2011; Desprat et al., 2013; Sicre et al., 2013; Castañeda et al., 2016). In fact, in the Adriatic Sea, HS1 was characterized by increased aridity and extremely cold conditions (Asioli et al., 2001) and some other records highlight distinct change in surface water temperatures, such as a two-step HS1 cooling (Sicre et al., 2013).

The present study provides the first centennial/multi-decadal time scale reconstruction of paleoenvironmental conditions across the last deglaciation, between 20 and 11 ka BP, in the South Adriatic Sea (SAS), combining terrestrial and marine biomarkers with calcareous plankton assemblages (coccolithophores and planktonic foraminifera). The sediment core ND14Q-AR2 used for this study was retrieved from the deepest part of the South Adriatic basin. This area provides an ideal location for high resolution paleoclimatic reconstructions because of thick deglaciation and Holocene sedimentary sequences and recurrent tephra layers for geochronological constraints (Siani et al., 2004, 2013; Lowe et al., 2007; Jalali et al., 2018; Cascella et al., 2019; Totaro et al., 2022). Terrestrial and marine biomarkers were used to infer environmental changes such as Sea Surface Temperatures (SSTs), in tandem with terrestrial input associated with humidity changes on adjacent lands (Jalali et al., 2018; Ternois et al., 2000). Recent studies have proven the value of cross-analysis of marine and terrestrial biomarkers to interpret multidecadal climatic variations contained in paleoclimate signals (Jalali et al., 2016, 2017, 2018; Schirrmacher et al., 2019). In fact, paired high-resolution marine and terrestrial biomarker records in the SAS over the last three millennia have shown the impact of North Atlantic Oscillation (NAO) and East Atlantic (EA) on SSTs centennial-scale variability (Jalali et al., 2018). On the

other hand, detailed calcareous plankton description from SAS are either scarce or mostly focused on planktonic foraminifera across the latest part of the deglaciation (Younger Dryas) to Holocene interval (Asioli et al., 1999, 2001; Capotondi et al., 1999; Sangiorgi et al., 2003; Favaretto et al., 2008; Piva et al., 2008; Narciso et al., 2012; Siani et al., 2013). In the same interval very few data exist on the coccolithophore assemblages (Giunta et al., 2003; Sangiorgi et al., 2003; Narciso et al., 2012; Cascella et al., 2019) and do not focus on the detail changes that occurred during the deglaciation. The study of core ND14Q-AR2 provides the first paleoenvironmental reconstruction of the deglaciation in the SAS that comprehends coccolith, planktonic foraminifera and biomarker analysis at high-temporal resolution to explore multidecadal changes at a regional scale during the deglaciation.

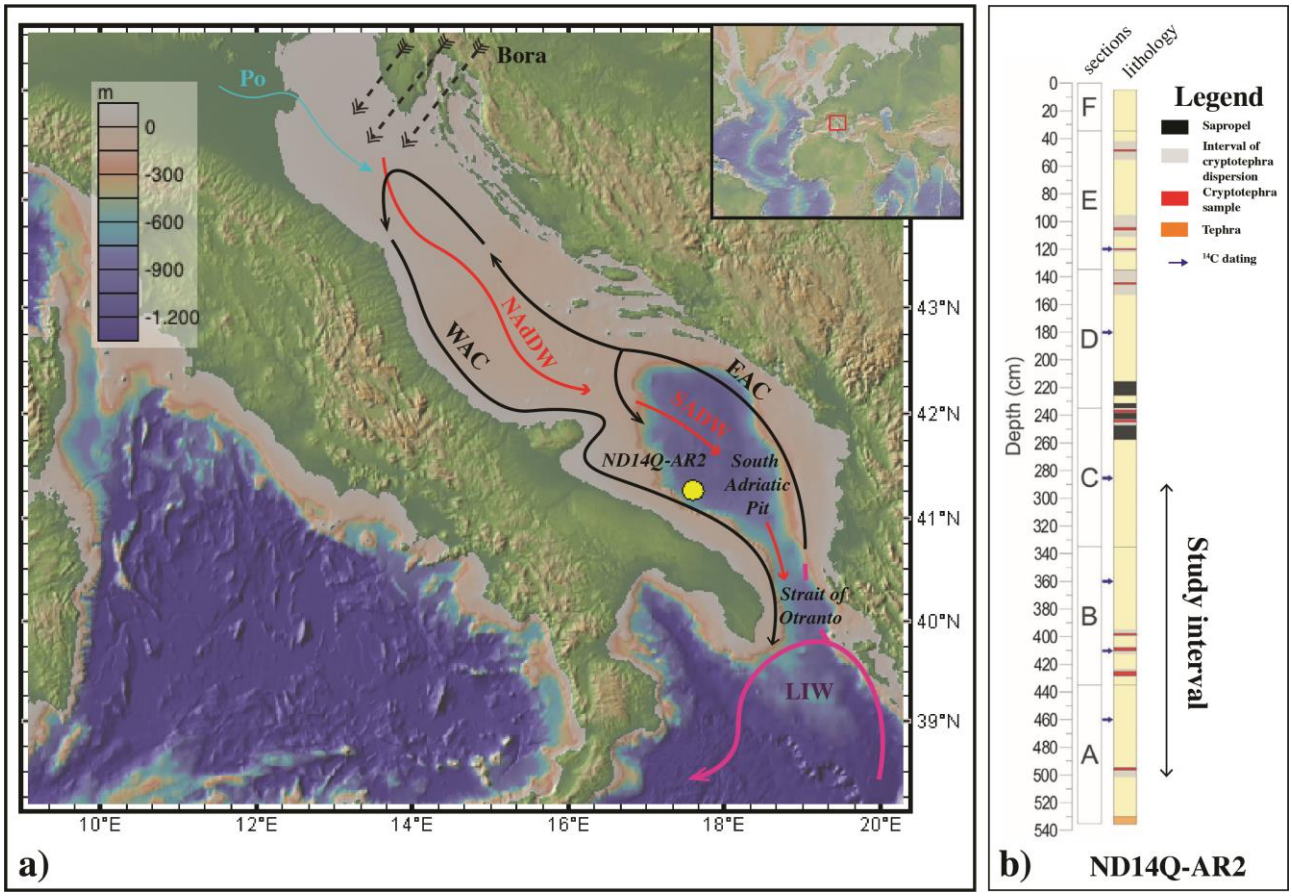

Fig. 1: a) Modern oceanographic circulation in the Adriatic Sea, bathymetry of the area and location of the core ND14Q-AR2 (yellow dot). Black lines, surface circulation: **EAC** (East Adriatic Current), **WAC** (West Adriatic Current). Purple lines, middle water circulation: **LIW** (Levantine Intermediate Water). Red lines, deep water circulation: **NAdDW** (North Adriatic Deep Water), **SADW** (South Adriatic Deep Water). b) Lithological log of core ND14Q-AR2 from Totaro et al. (2022). The black line represents the portion of the core studied here.

2. Study area

2.1. Oceanographic and climate setting

The Adriatic Sea is a semi-closed elongated basin located between the Balkans and the east coast of the Italian Peninsula, connected to the Mediterranean Sea through the Strait of Otranto (Fig.1a). The Adriatic bathymetry

is characterized by a shallow northern basin, with an average depth of ca. 35 m, which increases in the southern sector to an average depth of ca. 800 m (Ridente and Trincardi, 2002, 2006; Trincardi et al., 2007) and to about 1200 m in the deepest portion of the basin, the South Adriatic Pit (Artegiani et al., 1997). Surface water circulation in the Adriatic Sea is characterized by the cyclonic circulation conditions of the South Adriatic Gyre (SAG, Gačić et al., 1997), involving the East Adriatic Current (EAC) flowing northwards from the eastern margin of the Strait of Otranto, along the Balkan coast, and descending as West Adriatic Current (WAC), alongside the east Italian peninsula (Fig. 1a). The WAC, through freshwater discharges mostly from the Po River and subordinately by small rivers along the Italian coast, delivers low-salinity water southwards, together with suspended and dissolved substances enriching the basin with continental-derived nutrients (Lipizer et al., 2014). Intermediate waters, flowing between 200 and 600 m, are composed by the Levantine Intermediate Water (LIW) that flows in the Strait of Otranto from the Levantine Basin (Artegiani et al., 1997) (Fig. 1a). The deepest water mass is represented by a dense water mass flowing southward from the northern sector (Northern Adriatic Dense Water, NAdDW) sustained by Bora wind, blowing from the northwest during winter (Gačić et al., 2002; Turchetto et al., 2007). The NAdDW combines with the Southern Adriatic Dense Water (SADW) in the SAS (Fig. 1a), leading to one of the main source of the Mediterranean deep waters (Lascaratos, 1993; Pinardi and Masetti, 2000; Manca et al., 2002).

With regard to the atmospheric circulation, the Adriatic Sea is situated between the subtropical high-pressure zone and the mid-latitude westerlies belt (Orlić et al., 1992). Westerlies dominate most of the year, although during summer, the subtropical high-pressure zone step over and the cyclonic and anticyclonic disturbances of the westerlies belt almost disappear from the Adriatic (Orlić et al., 1992). These atmospheric influences, together with winter Bora winds, result in a typically Mediterranean climate characterized by stormy and relatively cold winter and hot and dry summer.

3. Materials and Methods

3.1. Core ND14Q-AR2

Core ND14Q-AR2, located in the southern Adriatic Sea (41°16' N, 17° 37' E), about 40 km from the Apulian coast (Fig.1a), was retrieved at 1013 m below sea level during the Next-Data 2014 expedition on board of the Italian R/V Urania. The coring was possible thanks to the NextData project, a scientific collaboration among several national research agencies, with the goal to acquire knowledge and know-how from climate archives in the Italian territory (http://www.nextdataproject.it/). The entire core is 540 cm long (Fig.1b), while the investigated section here extends from cm 285 to cm 505. Main lithology consists of gray/brown silty-clays, with ten interbedded cryptotephra layers and one tephra (Fig.1b). The adopted age model (Totaro et al., 2022) relies on 10 radiocarbon (^{14}C) AMS measurements and 6 tephra (cryptotephra and tephra) layers and was constructed using the Bayesian model with the Bayesian statistic software Bacon with the statistical package R (Blaauw and Christen, 2011).

3.2. Coccolith assemblage analysis

A total of 99 samples were prepared and analysed for quantification of coccolithophore assemblages at a sampling step of 2 cm over an interval ca. 220 cm long, with an average temporal resolution of ca. 80 yrs/sample. Samples were prepared following Flores and Sierro (1997) in order to estimate both the relative and absolute coccolith abundances. Quantitative analyses were performed using a polarized light microscope at 1000× magnification. At least 500 specimens were counted per sample. Reworked calcareous nannofossils were counted separately in the investigated fields of view and their relative % abundances determined against the 500 non-reworked coccoliths. The absolute abundances of taxa (Total N) expressed as the number of coccoliths per gram of dry sediment (Ng^{-1}) were calculated with the following equation:

$$\mathbf{N = n \times R^2 \times V \times r^{-2} \times g^{-1} \times v^{-1}}$$

where **N** is the absolute number of nannofossils per gram of dry sediment, **n** is the counted number of nannofossils in a random scanned area, **R** is the radius of the Petri dish, **V** is the volume of buffered water added to the weighted dry sediment, **r** is the radius of the visual field used in the counting, **g** is the gram of dry sediment, **v** is the volume of the pipetted sample (water and sediment) in the Petri dish.

Coccolith taxonomy mostly uses Young et al. (2003) and Jordan et al. (2004). In addition, the taxon *Emiliania huxleyi* was separated into two main morphotypes following size criteria: small *Emiliania* (SE) < 4µm and large *Emiliania* (LE) > 4µm (Colmenero-Hidalgo et al., 2002). Taxonomic subdivisions among gephyrocapsids follow Flores *et al.* (2000). The algebraic sum of *Calciosolenia* spp., *Discosphaera tubifera, Rhabdosphaera clavigera, Umbilicosphaera foliosa, Umbilicosphaera sibogae*, *Umbellosphaera* spp. and *Oolithotus* spp., i.e. taxa having preference for oligotrophic, tropical and sub-tropical waters (Winter and Siesser, 1994; Baumann et al., 2004; Boeckel and Baumann, 2004), is plotted as warm-water coccolith taxa (WWCT) and used as warm surface water proxy.

3.3. Biomarker analysis

Ninety-three samples were analysed for biomarkers at a sampling step of about 2 cm, with the exception of the bottom 10 cm where sampling step was increased to 4 cm. This resolution provides a temporal resolution of 1 sample every ca. 80 years, and 1 sample every ca. 160 years for the bottom 10 cm. A few grams of sediment were freeze-dried to extract lipids following Ternois et al. (2000). Both alkenones and n-alkanes were isolated from the total lipid extract by silica gel chromatography. A Varian CX 3400 gaschromatograph was used to quantify n-alkanes and alkenones after addition of 5 α-cholestane prior injection. Long-chain alkenones in open sea waters are known to be mainly produced by the coccolith taxon *Emiliania huxleyi*, the most abundant coccolithophore in the modern ocean (Paasche, 2002). The unsaturation index of C_{37} alkenones ($U_{37}^{k'}$) and calibration of Conte et al. (2006) were used to derive SSTs using the following equation:

$$T[C°] = -0.957 + 54.293\,[U_{37}^{k'}] - 52.894\,[U_{37}^{k'}]^2 + 28.321\,[U_{37}^{k'}]^3$$

High-molecular weight n-alkanes with an odd number of carbon atoms (Σ[C27]+[C29]+[C31]+[C33], hereafter named TERR-alkanes) produced by higher plants were used to estimate terrestrial inputs from the vegetation. These compounds are constituents of epicuticular wax of higher plants used by the vegetation to reduce water loss by evapotranspiration (Gagosian and Peltzer, 1986). The Average Chain Length (ACL) of

n-alkanes was calculated between C_{27} to C_{33} to assess past moisture conditions on land, based on the assumption that longer chains are synthetized by plants in response to limited water availability (Gagosian and Peltzer, 1986; Eglinton and Eglinton, 2008; Jalali et al., 2018)

3.4. Planktonic foraminiferal analysis

Planktonic foraminifera were identified in 101 samples at sampling step of 1 cm focused on the interval between 19.6 and 13.7 ka BP the average temporal resolution is of ca. 50 yrs/sample. The samples were dried in an oven at 50°C and washed with deionized water using a 63 μm mesh sieve. Quantitative analyses on planktonic foraminifera assemblage were carried out on 125 μm mesh sieved fractions. About 200-300 specimens of planktonic foraminifera were counted and identified in each sample to have a significant statistic. The taxonomic concepts and ecological inferences are based on Hemleben et al. (1989) and Pujol and Vergnaud-Grazzini (1995). Fifteen species of planktonic foraminifera were identified. Some planktonic species were grouped as follows: *Orbulina* spp. includes both *O. universa* and *O. suturalis*; *Globigerinoides quadrilobatus* includes *G. trilobus* and *G. sacculifer*; *Globigerinoides ruber* includes *G. gomitulus*; *Globigerina bulloides* includes *G. falconensis*; *Globigerinatella siphonifera* includes *G. calida.* Analyses discriminated between left and right coiling of *Globorotalia truncatulinoides, G. inflata, G. scitula* and *Neogloboquadrina pachyderma.* The data obtained were expressed in relative abundances (%).

A planktonic foraminiferal paleoclimate curve was constructed (Cita et al., 1977; Sanvoisin et al., 1993; Capotondi et al., 2016) from the algebraic sum of warm-water species percentages (expressed as positive values) and cold-water species percentages (expressed as negative values), featuring ecological preferences and modern habitat characteristics as reported in Hemleben et al. (1989), Rohling et al. (1993), and Pujol and Vergnaud-Grazzini (1995). Warm-water species include *G. ruber* (white and pink varieties), *G. quadrilobatus*, *G. siphonifera* and *O. universa*. Cold-water species encompass *G. bulloides, Globigerinita glutinata, Turborotalita quinqueloba, G. inflata, G. scitula, G. truncatulinoides* left coiled and *N. pachyderma* right coiled. Here, we only show the abundance profile of *G. truncatulinoides* left coiled. Negative and positive values of the curve correspond to the cold and warm surface waters, respectively.

3.5. X-ray Fluorescence (XRF)

Bulk elemental geochemical composition of core ND14Q-AR2 was measured at the CORELAB laboratory of the University of Barcelona with an Avaatech XRF core scanner. The sediment core was measured at 1 cm resolution with excitation conditions of 10 kV, 0.5 mA and 10 s for major elements. For the scope of this paper only the log-ratio of K and Al is shown. Log-ratio of element intensities has demonstrated to provide the most easily interpretable signal of relative changes in chemical composition (Weltje and Tjallingii, 2008).

4. **Results**

4.1. Coccolithophore assemblage

Total N values range between 2 x 10^8 coccoliths/g and 2.7 x 10^9 coccoliths/g, with an average of 1 x 10^9 coccoliths/g (Fig. 2a). In the lower part of the record the coccolith abundance is extremely low, while it gradually increases at ca. 17 ka BP and has highest values from 15 ka BP till the top of the record, with a brief decrease at 12 ka BP (Fig. 2a). SE represents the most abundant taxon, with percentages lying between 60 and 80 % (Fig. 2b). The relative abundance of LE is generally not higher than 10% although pronounced increases occur at 16.8 ka BP, 15.9 ka BP, and between 14.4 and 13.6 ka BP (Fig. 2c). *Coccolithus pelagicus* ssp. *pelagicus*, generally representing <10% of the assemblage, shows relative abundances of about 15% during the 18-16 ka BP interval (Fig. 2d). Reworked coccolith taxa show a similar relative abundance pattern, with high values in the older part of the interval and declining at 18-16 ka BP (Fig. 2e). Although not a dominant component of the assemblages (never > 15 %), *Florisphaera profunda* exhibits very low percentages (generally < 3%) along the whole record, while rising with fluctuating abundances, between 14.8 and 13 ka BP (Fig. 2f). Among the less abundant taxa, *Syracosphaera* spp. (*Syracosphaera histrica* and *Syracosphaera pulchra*) and *Helicosphaera carteri* show a similar pattern of distinct decrease from higher relative abundances in the oldest part of the record (ca. 20-15.7 ka BP) to a decrease onward, with an isolated peaking values at ca. 14.8 ka BP (Fig. 2g, h). The WWCT indicate very low abundances throughout the core, generally < 4 %, with increasing values between 14.8 and 12.3 ka BP, and from 11.5 ka BP up to the top of the studied interval (Fig. 2i). Other taxa of minor abundances, not exceeding 3% of the assemblage, are not shown. They include *Coccolithus pelagicus* ssp. *braarudii*, *Coccolithus pelagicus* ssp. *azorinus*, *Braarudosphaera bigelowii*, *Calcidiscus leptoporus* ssp. *small* (3–5 µm), *C. leptoporus* ssp. *leptoporus* (5–8 µm), *C. leptoporus* ssp. *quadriperforatus* (8–10 µm), *Ceratolithus* spp., *Helicosphaera hyalina*, *Gephyrocapsa* spp., *Gladiolithus flabellatus, Umbilicosphaera hulburtiana, Pontosphaera* spp., *Scyphosphaera* spp.

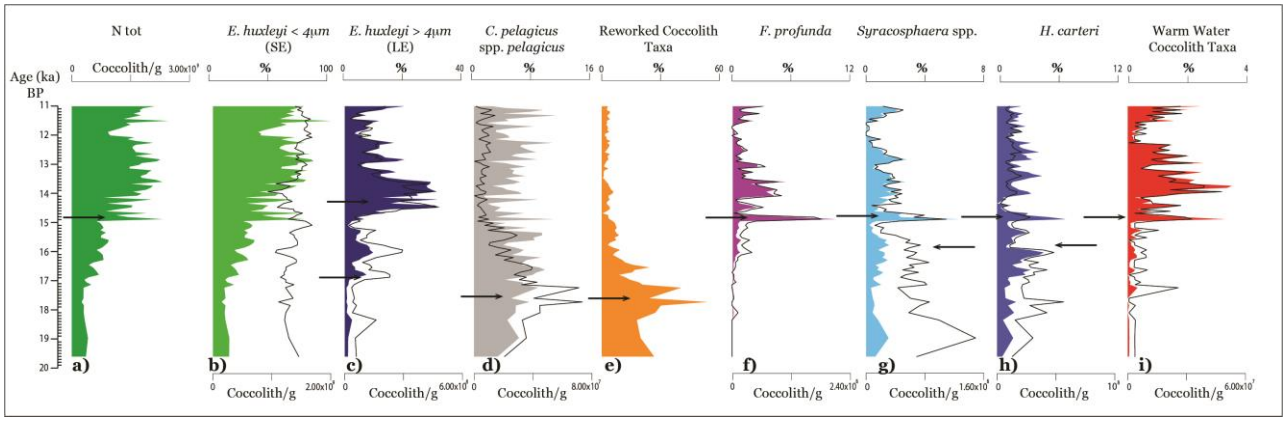

Fig. 2: Coccolithophore assemblage variations from core ND14Q-AR2 (thick lines relative abundances, %; filled area absolute abundance, Coccolith/g). Reworked coccolith taxa are plotted as relative abundance (%). Total N: total coccolithophore abundance variations. Black arrows indicate significant increases/decreases in abundances as signalled in the text.

4.2. Biomarker data

The SST reconstruction reveals multidecadal variability over the 11-20 ka BP interval featuring rapid surface hydrological changes (Fig. 3a). Values between 20 and 17 ka BP, where temporal resolution is lower, range

between 19 and 12°C. Values decrease from 16 to 10 °C between 17 to 15.5 ka BP, to reach a minimum value of 10°C at 16 - 15 ka BP (Fig. 3a). A second cold interval (ca. 11°C) is also recorded between 12 and 11 ka BP (Fig. 3a). Between these cold periods (15 to 12.5 ka BP) SST gradually rises to nearly 16°C (Fig. 3a). TERR-alkane concentrations along the core ND14Q-AR2 do not show a clear trend but rapid shifts highlighting short-term terrestrial inputs to the site (Fig. 3b). ACL values show relatively high values during the entire interval (nearly 30). Lower ALC appeared to coincide with high TERR-alkanes (Fig. 3c).

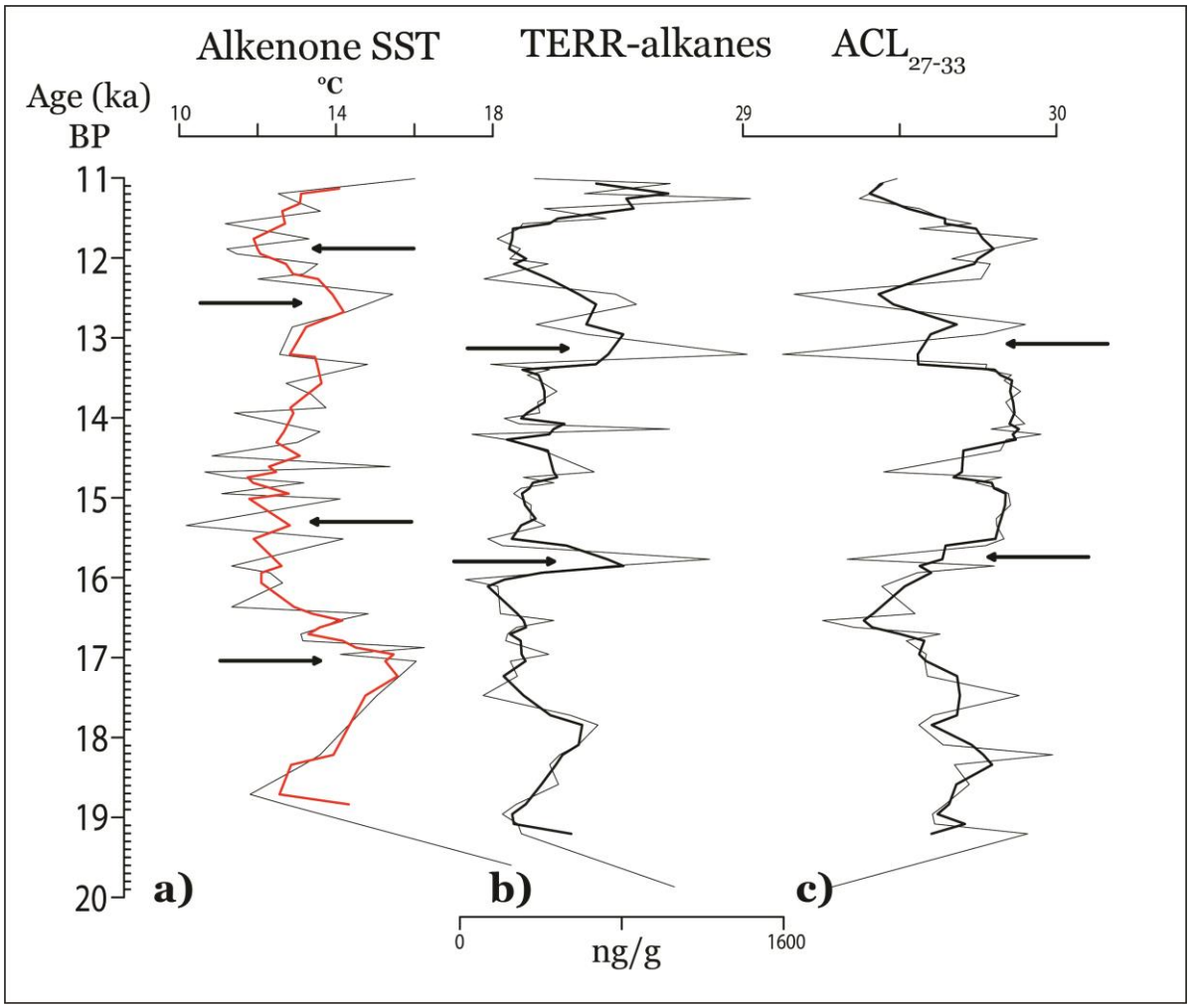

Fig. 3: Variations through time of marine (a) and terrestrial (b, c) biomarkers from core ND14Q-AR2. Thick lines 3-points average. Black arrows indicate significant increases/decreases in abundances as signalled in the text.

4.3. Planktonic foraminiferal assemblage

Planktonic foraminifera are well preserved and diversified. Assemblages are mainly represented by *N. pachyderma* right coiled (rc) and characterized by three intervals of lower values between 19.01-18.6, 17.7-17.1 and 14.7-14.07 ka BP (Fig. 4a). *Globigerinita glutinata*, *G. scitula* and *T. quinqueloba* were identified till ca. 14.5 ka BP (Fig. 4b, c, d). *G. glutinata* abundance profile is characterized by two stepwise decreases at 17.1 and 14.5 ka BP (Fig. 4b); *G. scitula* abundances fluctuate between 5 and 20% and reach maximum values between 15.42 and 14.8 ka BP before an important decrease (Fig. 4c). *Turborotalita quinqueloba* shows a

prominent peak at 17.2 ka BP and a progressive decrease with time opposed to the *G. scitula* abundances (Fig. 4d). *Globigerina bulloides* is present throughout the studied section and shows two major peaks (ca. 30%) at 14.1 ka and 16.2 ka BP (Fig. 4e). *Globigerinoides ruber* white shows a characteristic increase in abundance from ca. 3% to ca. 45% at 14.9 ka BP (Fig. 4f). *Globorotalia inflata* is only present in the uppermost part of the study section between 13.6 and 15.3 ka BP with abundance lying between 2 and 18% (Fig. 4g). *Neogloboquadrina dutertrei*, *Orbulina* spp., *G. siphonifera*, *G. rubescens*, *G. quadrilobatus*, *G. ruber* pink and *G. truncatulinoides* left coiled occasionally reach values between 3 to 6 %. The planktonic foraminiferal paleoclimatic curve shows a main shift from cold to warm conditions at ca. 15 ka while the older part shows relatively constant values except for two warmer intervals at 18.7-19.1 and 17.2-17.8 ka BP (Fig. 4i).

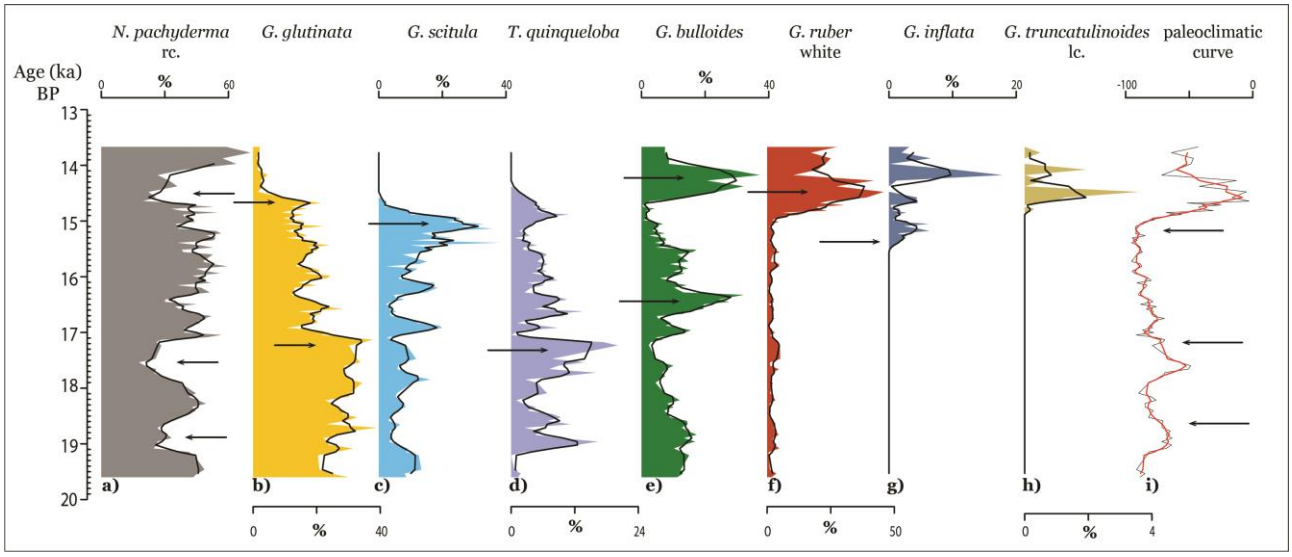

Fig. 4: Foraminifera assemblage relative abundance from core ND14Q-AR2 (%; thick line 3-points average), and foram-based paleoclimate curve (thick line 3 points average). Black arrows indicate significant increases/decreases in abundances as signalled in the text.

5. **Discussion**

5.1. Surface water conditions in the SAS

5.1.1. Last Glacial Maximum (LGM)

Comparison between alkenone-derived SSTs and WWCT relative abundances through the record reveals several millennial-scale climate phases (Fig. 5b, c). Within the uncertainty of age models, well-known climate period from the Last Glacial Maximum to the Early Holocene period that are reflected in the Stadial and Interstadials of the Greenland ice core oxygen isotope record (Rasmussen et al., 2014) (Fig. 5a), match with SST changes as expected from ocean and atmospheric linkages with the North Atlantic region. They include the latest part of the Last Glacial Maximum (LGM, 20-17.1 ka), the Heinrich Stadial 1 (HS1, 17.1-14.9 ka), the Bølling-Allerød period (BA, 14.9-12.3 ka) and the Younger Dryas (YD 12.3-11 ka).

SSTs during the LGM indicate a marked cooling (Fig. 5b). The low temporal resolution of the SST signal during this time interval, due to insufficient amount of alkenones, is consistent with the low absolute abundances of *E. huxleyi* (Fig. 2b, c) pointing out non-favourable growth conditions. The WWCT signal and

planktonic forams paleoclimate curve provide a more detailed picture of the surface water conditions in the SAS during the LGM and notably the extremely low and negative values respectively, witnessing cold surface water conditions (Fig. 5c, e). A warm interval starts at ca. 17.6 ka BP according to the SSTs, WWCT and the planktonic forams paleoclimate curve, and reaches 16°C between 17.5-17.1 ka BP (Fig. 5b c, e). This episode seems to be coeval with lighter $\delta^{18}O$ in Greenland ice cores indicating warmer temperature in the earlier GS-2.1a (Fig. 5a). During the LGM, the high but decreasing abundances of reworked coccoliths (Fig. 6i) suggests enhanced erosion in the borderland area and continental detrital inputs to the core location (Flores et al., 1997; Bonomo et al., 2014, 2016; Maiorano et al., 2016). At that time of lower sea level, the northern Adriatic basin was almost completely subaerially exposed and the Po river mouth likely located closer to the ND14Q-AR2 site (Correggiari et al., 1996; Vai and Cantelli, 2004). Synchronous low total coccolith abundances indicate that cold and turbid surface waters were not favourable to coccolith growth (Fig. 5i). Coeval increased *G. glutinata* and *T. quinqueloba* (Fig. 6h) seems to support the occurrence of land-derived nutrient in surface waters (Cita et al., 1977; Corselli et al., 2002; Geraga et al., 2008; Jonkers et al., 2010; Margaritelli et al., 2018).

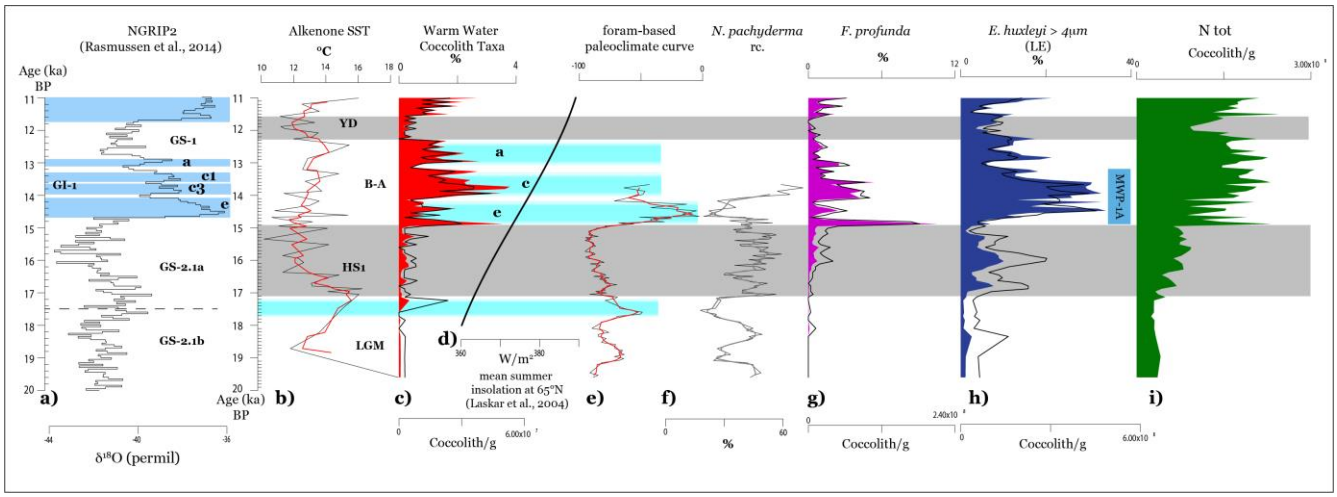

Fig. 5: Core ND14Q-AR2 records: a) Greenland $\delta^{18}O$ (Rasmussen et al., 2014); b) alkenone base SST (red line represents a 3-points running average); c) warm coccolith taxa (WWCT) distribution pattern (black line, relative abundances, %; colored area, absolute abundances, Coccolith/g); d) summer insolation curve (Laskar et al., 2004); e) foram-based paleoclimatic curve (thick line, 3 points average); f) *N. pachyderma* rc relative abundances (%; dark lines, 3-points average); g) *F. profunda* distribution pattern (black line, relative abundances, %; colored area, absolute abundances, Coccolith/g); h) *E. huxleyi* > 4 μm distribution pattern (black line, relative abundances, %; colored area, absolute abundances, Coccolith/g); i) total coccolithophore abundance variations. **LGM** (Last Glacial Maximum); **HS1** (Heinrich Stadial 1, grey bar); **B-A** (Bølling-Allerød); **YD** (Younger Dryas, grey bar); **GS** (Greenland Stadial and sub events 2.1a, b); **GI** (Greenland Interstadial and sub events: **a, c, e**); **MWP-1A** (Melt Water Pulse).

5.1.2. Heinrich Stadial 1 (HS1)

313 The SST decline at 17.1 ka (Fig. 5b) reflects the climate response of the Adriatic Sea to the onset of the HS1
314 event, in agreement with earlier studies in the Mediterranean (Cacho et al., 1999; Sierro et al., 2005; Kotthoff
315 et al., 2011). SST cooling during Heinrich events in the Mediterranean has been linked to cold water inflow
316 from the Atlantic Ocean (Cacho et al., 1999, 2001) combined with intensified cold winds in winter (Rohling
317 et al., 1998; Cacho et al., 2000). The HS1 is identified in our core between 17.1 and 14.9 ka by a ~6°C SST
318 drop to the lowest values of the record (10°C) at 16-15 ka (Fig. 5b). The WWCT and foraminiferal paleoclimate
319 curves do not show remarkable changes at the onset of HS1 (Fig. 5b) while conversely, HS1 cooling is clearly
320 manifested by an abrupt increase of % *N. pachyderma* rc (Fig. 5f), a progressive increase of polar-subpolar
321 taxon *G. scitula* (Ortiz et al., 1996; Schiebel et al., 2002) (Fig. 6b). The occurrence of *N. pachyderma* rc is
322 indicative of cold and eutrophic conditions (Hemleben, et al., 1989; Pujol and Vergnaud-Grazzini, 1995;
323 Rigual-Hernández et al., 2012). Increase abundances of opportunistic species *G. bulloides*, during this interval
324 (Fig. 6c), further support enhanced nutrient availability in the upper surface ocean, most likely promoted by
325 seasonal winter mixing and/or continental runoff (Cita et al., 1977; Schiebel et al., 2001; Corselli et al., 2002;
326 Geraga et al., 2008; Jonkers et al., 2010; Margaritelli et al., 2018, 2020). In the Adriatic Sea, several studies
327 reported the occurrence of *N. pachyderma* rc during the cold events of the last deglaciation (Asioli et al., 2001;
328 Trincardi et al., 2007; Favaretto et al., 2008; Piva et al., 2008; Siani et al., 2010; Narciso et al., 2012). This
329 taxon has also been found during HS1 in the Ionian Sea (Geraga et al., 2008), in the Sicily Channel (Sprovieri
330 et al., 2003) and in the North Aegean Sea (Kotthoff et al., 2011). Finally, cold-water species *G. inflata* (De
331 Castro Coppa et al., 1980; Pujol and Vergnaud-Grazzini, 1995) combined to highest values of *G. scitula* (Ortiz
332 et al., 1996; Schiebel et al., 2002) between 15.3 and 14.9 ka (Fig. 6f, b) points to the coldest phase of HS1
333 (Fig. 6a).
334 During HS1, coccolith assemblages are also characterized by increased LE abundances (Fig. 5h). This
335 morphotype is absent in present day assemblages with the exception of cold ocean waters in the Arctic and
336 Subarctic regions (Hagino et al., 2005; Flores et al., 2010). Its presence in the western Mediterranean basin
337 during the late Pleistocene and Holocene has been used to capture cold/fresher surface water masses during
338 HS events (Colmenero-Hidalgo et al., 2002, 2004; Flores et al., 2010; Ausín et al., 2015; Di Stefano et al.,
339 2015; Bazzicalupo et al., 2018). The LE morphotype has never been documented before in the central
340 Mediterranean nor in the Adriatic Sea, where its ecological behaviour and its potential value as
341 ecostratigraphical pattern is unknown. Its occurrence during HS1 in our core supports the signature of cold-
342 fresher surface water most probably linked to meltwater from local continental ice and their delivery by the Po
343 River. Highest relative abundances of this taxon are also recorded in younger sediment layers of the core and
344 will be discussed in the following sections.
345 The HS1, as identified at ND14Q-AR2, matches well with the cold portion of Greenland Ice counterpart GS-
346 2.1a (Fig. 5a). The SST decrease in the later phase of the HS1 is in good agreement with the extreme cooling
347 in the eastern Mediterranean and Red Sea (Arz et al., 2003; Castañeda et al., 2010, 2016).

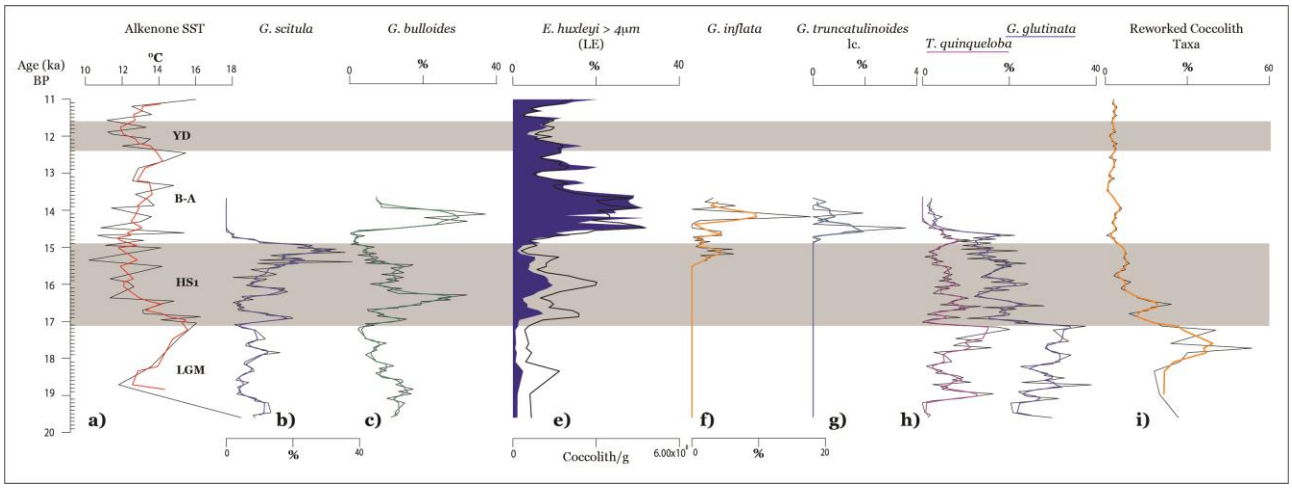

Fig. 6: Core ND14Q-AR2 records: a) alkenone base SST (red line represents a 3-points running average); b, c, f, g, h) foraminifera taxon distribution patterns (%; dark lines, 3-points average); e) *E. huxleyi* > 4 μm distribution pattern (black line, relative abundances, %; colored area, absolute abundances, Coccolith/g); i) reworked coccolith taxa distribution pattern (black line, relative abundances, %; orange line, 3-points average). **LGM** (Last Glacial Maximum); **HS1** (Heinrich Stadial 1, grey bar); **B-A** (Bølling-Allerød); **YD** (Younger Dryas, grey bar).

5.1.3. The Bølling-Allerød (B-A)

The B-A interstadial spans between 14.9 and 12.3 ka BP, as revealed by the general increase of WWCT and the gradual alkenone-SST rise from 11 to 15.5 °C (Fig. 5b), as well as by a positive shift of the foraminifera paleclimatic curve (Fig. 5e). During the B-A event, the WWCT exhibit three centennial-scale oscillations that are partially registered by planktonic foraminiferal curve as well (Fig. 5c, e). These three warmings are nearly contemporaneous to the succession of warm intervals known as GI-1e, c1-3, a (Fig. 5a) (Rasmussen et al., 2014). These high frequency fluctuations were also previously observed in other planktonic foraminiferal assemblage records from the SAS (Asioli et al., 2001; Siani et al., 2010).

During the B-A we observe an increase in the abundance of the deep dwelling taxon *F. profunda* (Fig. 5g), pointing to seasonal stratification and deep nutricline/thermocline conditions (Molfino and Mcintyre, 1990; Beaufort et al., 1997; Di Stefano and Incarbona, 2004; Balestra et al., 2008) likely related to gradual increase of insolation and related surface water warming (Fig. 5d) (Beaufort et al., 1997, 2001). Indeed, the increase of Total N (Fig. 5i) suggests ameliorated surface water conditions for the coccolithophore assemblage i.e., warmer surface waters and seasonal nutrients availability, likely related to seasonal mixing. The strong increase of *G. bulloides* (Fig. 6c) together with the peaks in abundance of *G. truncatulinoides* and of *G. inflata* (Fig. 6f, g), suggest a deep vertical mixing during the winter season in the study sites at the onset of the B-A, with a strong advection of nutrients from the deeper layers to the surface (Schiebel et al., 2001; Margaritelli et al., 2020).

LE occurrences rising between 14.7 and 13.4 ka BP is also observed. As mentioned before the distribution of this taxon is not known in the central Mediterranean but well documented in the western Mediterranean throughout this interval and has been related to the inflow of colder and fresher Atlantic water in the Alboran

Sea, likely deriving from iceberg melting (Colmenero-Hidalgo et al., 2002, 2004; Flores et al., 2010; Ausín et al., 2015; Bazzicalupo et al., 2018). Given its ecological preference, the LE increase in our record seems to point out to cold freshwater outburst in the SAS through the Po River due to Alpine and Apennine ice sheets melting resulted from ameliorated climate in the North Atlantic (as revealed by Greenland ice). Indeed previous data provide evidence of ice melting in the Alps mountains surrounding the Adriatic basin and subsequent increased run off of the Po River (Combourieu-Nebout et al., 1998; Asioli et al., 2001). This hydrological episode recorded in the SAS would reflect the more global ice melt event known as the MWP-1A (Bard et al., 1996; Fairbanks et al., 2005) (Fig. 5h), occurring around 14 ka BP (Liu and Milliman, 2004; Stanford et al., 2006). Altogether, our results suggest that the LE may be a valuable indicator of meltwater episodes into the SAS.

A closer look of the centennial scale variability shows that the major peak of *G. bulloides* and *G. inflata* occurring between 14.5 and 14.0 ka BP coincides with low relative abundances of LE (Fig. 6e, f). This opposite behaviour between taxa might feature decadal-scale shifts from freshwater driven stratified conditions (increase of LE) to cold and strong winds allowing for strong water column mixing and higher surface water nutrients (increase of *G. inflata* and *G. bulloides*).

5.1.4. Younger Dryas (YD)

Between 12.3 and 11.6 ka BP, alkenone SSTs show an abrupt cooling from 15.5 °C to values oscillating between 11-13°C (Fig. 5b) evidencing the return to cold water conditions of the YD period in the Mediterranean Sea (Cacho et al., 1999; Asioli et al., 2001; Di Stefano and Incarbona, 2004; Siani et al., 2010; Kotthoff et al., 2011; Sicre et al., 2013; Martrat et al., 2014). The coeval low relative abundances of WWCT are consistent with surface water cooling at the time of the GS-1 in Greenland ice (Fig. 5a).

5.2. Terrestrial inputs to the SAS

5.2.1. Terrestrial inputs during the HS1

Climate variability on land can be derived from ACL and TERR-alkanes content of the sediment. These biomarker proxies produced by higher plants allow to diagnose moisture conditions (Gagosian and Peltzer, 1986; Sicre and Peltzer, 2004) and have been successfully used for paleoclimate reconstructions in the Mediterranean (Jalali et al., 2016, 2017, 2018). K/Al ratio provides a complementary information on detrital riverine discharge (Frigola et al., 2008; Nieto-Moreno et al., 2011; Rodrigo-Gámiz et al., 2011; Martinez-Ruiz et al., 2015) Indeed, the northern Mediterranean regions are a major source of illite. River-derived increase of illite supply leads to higher K/Al ratios in the sediments during humid intervals (Martinez-Ruiz et al., 2015). The relatively high ACL values (Fig. 7b) suggest prevalent arid conditions on adjacent land and catchment basins, in agreement with the dominance of desert and semidesert vegetation type during the deglaciation in the central Mediterranean (Combourieu-Nebout et al., 1998; Magri and Sadori, 1999; Desprat et al., 2013). This general trend is interrupted by short humid phases as indicated by rapid ACL decrease (Fig. 7b). These

brief periods are generally accompanied by peaking TERR-alkanes, that might suggest a link with increased river run-off (Fig. 7a).

Of particular interest is a two-phase structure of HS1 portrayed by HS1a (17.1-15.9 ka BP) and HS1b (15.9-14.9 ka BP) (Fig. 7) not previously identified in the SAS. Low ACL values during HS1a suggest relatively humid conditions, while concurrent low TERR-alkanes are indicative of reduced higher plant material export to the SAS (Fig. 7d). Concomitant high values of K/Al ratio in the sediment point out to enhanced riverine discharge under relatively wet conditions (Fig. 7c). Abundance peak of reworked coccolith taxa during HS1a seems to support enhanced detrital inputs in the SAS (Fig. 7d). Altogether these data suggest enhanced delivery of detrital inputs with a lower contribution of higher plant with lower ACL, likely from an Alpine source. In addition, the herbivorous opportunistic planktonic foraminifera *G. bulloides,* often associated with high continental runoff (Pujol and Vergnaud-Grazzini, 1995; Rohling et al., 1997; Schiebel et al., 1997; Thiede et al., 1997; Capotondi et al., 2004; Schmidt et al., 2004; Principato et al., 2006) is also abundant (Fig. 7e) confirming enhanced continental input during HS1a. In contrast, during HS1b, ACL pattern shifts to higher values suggesting reduction in moisture availability on land (Fig. 7b). The low K/Al ratio during HS1b well supports reduced river input (Fig. 7c) as well as low TERR-alkanes (Fig. 7a).

Between HS1a and HS1b, peaking TERR-alkanes and low ACL (15.8 ka BP, Fig. 7a) suggests enhanced transport of higher plant derived material to the SAS, grown under humid conditions. The concomitant increase of LE abundances suggests a link with the supply of cold fresher waters (Fig. 7f). An almost identical event in the calcareous nannofossil assemblage has been identified in the western Mediterranean (Bazzicalupo et al., 2018) in the middle of the HS1, during a phase of increased melt water in the North Atlantic and/or in the Mediterranean via the Rhone River caused by Eurasian/Alps Ice Sheet complex melting (Cacho et al., 1999; Sierro et al., 2005; Frigola et al., 2008; Melki, 2011). The brief fresh water supply seen at our core location between HS1a and HS1b can thus reasonably be assigned to Alpine and Apennine melting ice (Asioli et al., 2001; Storms et al., 2008). The imprint of the short-lived episode in the middle of HS1 is also seen in the western Mediterranean (Martrat et al., 2014; Hodell et al., 2017) and in the Gulf of Cadiz (Sierro et al., 2020) showing lighter seawater $\delta^{18}O$ and warmer SST.

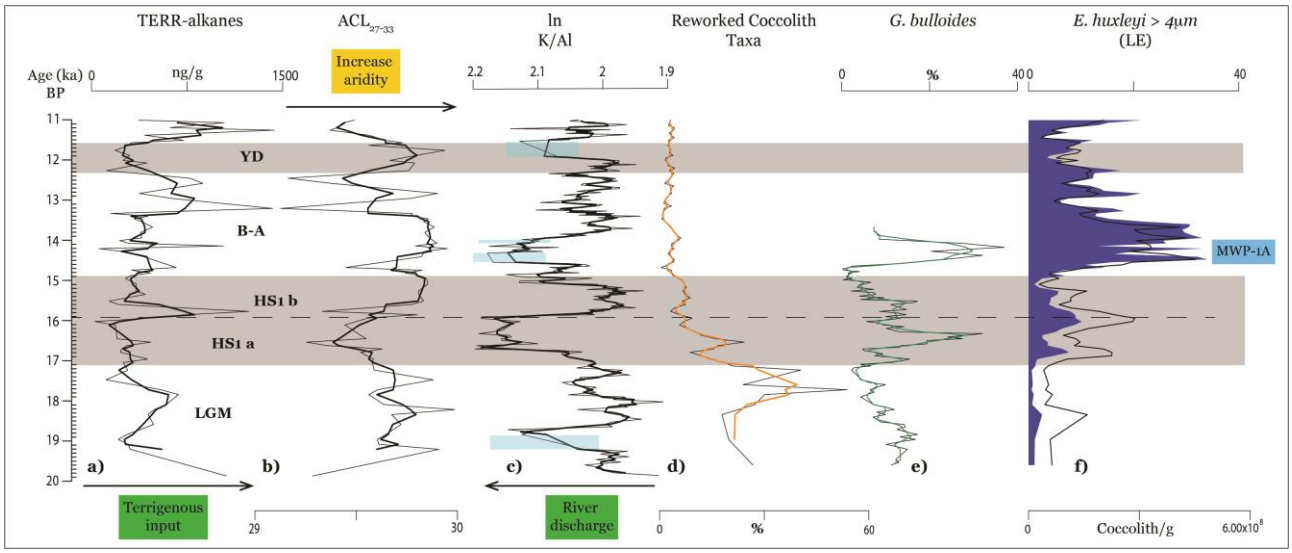

Fig. 7: Core ND14Q-AR2 records: a, b) terrestrial biomarker (TERR-alkanes and ACL_{27-33}; thick lines 3-points average); c) K/Al log ratio (thick line 3-point average, azure areas represents tephra layers levels removed from the figure to facilitate the observation); d) reworked coccolith taxa distribution pattern (black line, relative abundances, %; orange line, 3-points average); e) *G. bulloides* distribution pattern (%; dark lines, 3-points average); f) *E. huxleyi* > 4 μm distribution pattern (black line, relative abundances, %; colored area, absolute abundances, Coccolith/g). **LGM** (Last Glacial Maximum); **HS1** (Heinrich Stadial 1, grey bar); **B-A** (Bølling-Allerød); **YD** (Younger Dryas, grey bar); **MWP-1A** (Melt Water Pulse).

5.2.2. Terrestrial inputs during the B-A and YD.

During the earlier phase of B-A (14.9-13.4 ka BP), ACL values were generally lower (Fig. 7b) whereas TERR-alkanes show fluctuating values, indicating drier conditions on land. This finding is in apparent disagreement with the general indication of wetter climate conditions on land during the B-A, in contrast to HS1 and YD, based on central Mediterranean pollen records (Combourieu-Nebout et al., 1998; Magri and Sadori, 1999; Asioli et al., 2001; Desprat et al., 2013). However, it seems consistent with evidence of relatively warm climate and limited water availability, as suggested by dominant semi-desert plant remains in the central Mediterranean (Pollen Zone PZ2 between 13.7 and 13.1 ka BP, Desprat et al., 2013). Relatively high concentrations of the steppe taxon *Artemisia* (up to 30%) during the early stage of the B-A are also reported in the SAS (labelled as GI-1 e-d in Asioli et al., 2001).

The most recent part of B-A (13.4-12.3 ka BP) is characterized by two TERR-alkane increases concomitant with low ACL-values suggesting increased moisture availability (Fig. 7b). This increased humid local condition is well known throughout the Mediterranean as a major attribute of climate ameliorating in the basin (Combourieu-Nebout et al., 1998; Magri and Sadori, 1999; Combourieu Nebout et al., 2009; Fletcher et al., 2010; Desprat et al., 2013). The B-A interval ends with an increase of ACL indicating drier conditions again supported by evidence of prevailing dry conditions in the Mediterranean during the YD (Combourieu-Nebout et al., 1998; Fletcher and Sánchez Goñi, 2008; Combourieu Nebout et al., 2009; Fletcher et al., 2010; Desprat et al., 2013).

5.3. The Two-phase structure of the HS1

Our results in the Adriatic Sea reinforce the two-fold structure of HS1 found in many records around the world (Huang et al., 2019 and references therein), yet the forcing and physical mechanisms at play are still debated. Currently, in the central Mediterranean the detailed structure of HS1 is poorly documented and few records reported on prolonged aridity in the region across the interval embracing HS1 (Combourieu-Nebout et al., 1998; Asioli et al., 2001; Desprat et al., 2013), although some authors did not detail different phases within the HS1.

The distinct two-phase structure in our core, however, are mainly fingerprinted by terrestrial proxies that appear to reflect freshwater delivery in the SAS due to ice melting from the Alps mountains. A similar pattern, within the limit of comparing different age models, was also observed in the Alboran Sea (Fig. 8b)

(Bazzicalupo et al., 2018) and in the north-western Iberia margin (Fig. 8a) (Naughton et al., 2009, 2016; Voelker et al., 2009) during the HS1a, although well recorded in the marine proxies as well, similarly related to freshwater arrival. A shift in the European moisture source distribution was also inferred during HS1 based on evidences in the Black Sea (Kwiecien et al., 2009) and in the Aegean Sea (Kotthoff et al., 2011).

The SAS is under the influence of both mid-latitude westerlies wind belt and the subtropical high-pressure zone (Orlić et al., 1992). Moister conditions during the HS1a are likely related to the strength and latitudinal position of the westerly winds, with their southern position leading to relatively wetter conditions in southern Europe and in the Mediterranean region.

At the onset HS1 cold and fresh water from ice sheet melting was released in the North Atlantic, affecting the surface ocean circulation (Bond et al., 1992; Stanford et al., 2011). Subsequent collapse of the AMOC, diminished transport of warm and moist from low to high latitudes (Rahmstorf, 1994). This alteration of the AMOC resulted in North Atlantic/western Europe cooling (e.g. Seidov and Maslin, 1999; McManus et al., 2004). The associated southward displacement of the ITCZ and moisture transport to mid-latitudes resembles the negative NAO state (Trigo et al., 2004). Variability in precipitation and flood activity in the Alpine region and the northern catchment basin of the SAS have been related to the NAO variability (Bartolini et al., 2009; Wirth et al., 2013). In the eastern Mediterranean, Castañeda et al. (2016) (Fig. 8f) describes a two-phase HS1 nearly synchronous with core ND14Q-AR2: HS1a (c.a. 17.5-16 ka BP) characterized by relatively warmer SSTs and HS1b (16-14.5 ka BP) corresponding to colder and driest conditions on land, which is in good agreement with the HS1 interval in our core (Fig 8e, f). Huang et al. (2019) hypothesized a southward migration of the ITCZ reaching its southernmost position during the HS1b in agreement with climate modelling highlighting the southward shift of the ITCZ as the AMOC weakened (Kageyama et al., 2009). During HS1b, colder conditions in the Adriatic Sea are consistent with those of the easternmost Mediterranean (Fig. 8f) (Essallami et al., 2007; Castañeda et al., 2010, 2016) and with the weakest Asian monsoon (Fig. 8g) (Cheng et al., 2016; Huang et al., 2019) pointing to a linkage with the tropical Northern Hemisphere climate. Colder SSTs likely caused a further weakening of the AMOC (Huang et al., 2019) leading a southernmost position of the ITCZ (Deplazes et al., 2013; Zhang et al., 2014) explaining drier conditions in the northern-low to middle latitudes during the HS1b (Huang et al., 2019). The comparison between the Adriatic Sea, eastern Mediterranean and Southern-central Asian domain (Fig. 8) provides evidence of a mid- and low-latitudes reorganization of the atmospheric circulation during HS1 associated with the AMOC weakening.

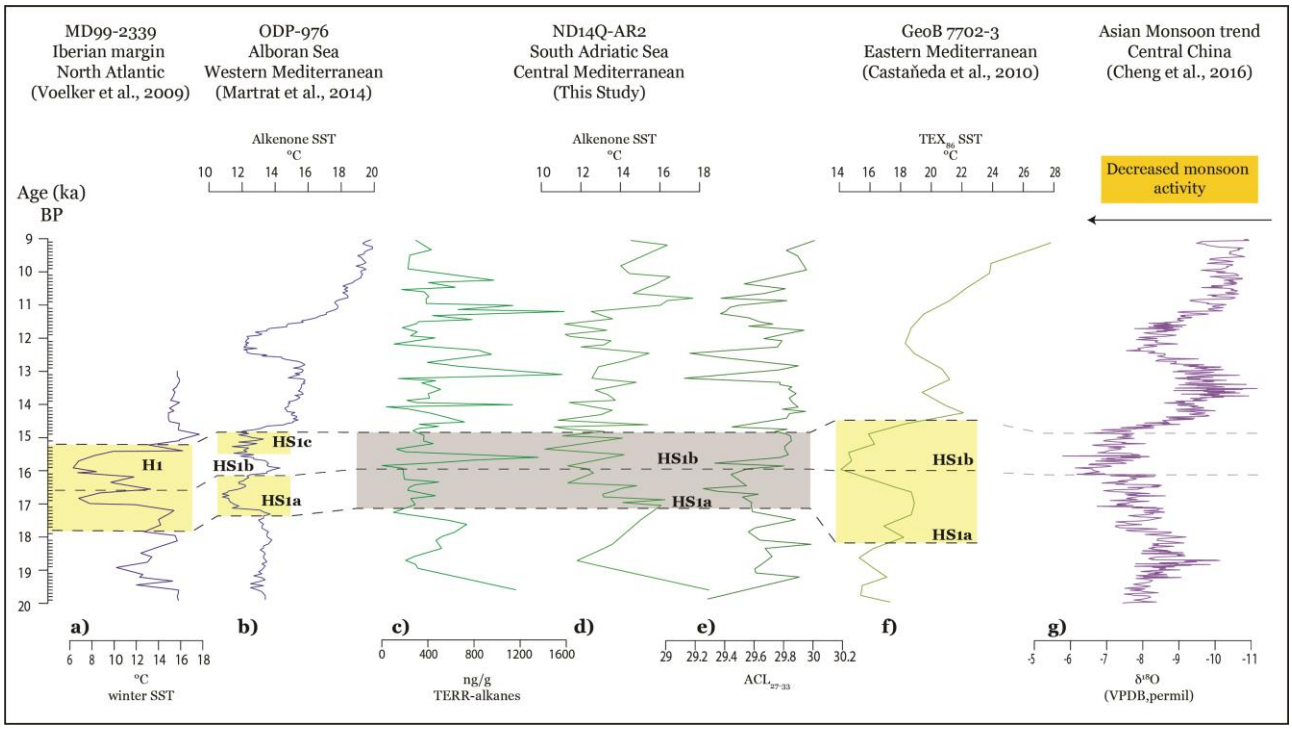

Fig. 8: Comparison of climate records across the Last Deglaciation in the Northern Hemisphere. a) Forams-based MAT winter SST curve from Core MD99-2339, Iberian Margin, North Atlantic (NA) (Voelker et al., 2009); b) Alkenone SST curve from ODP Core 976, Alboran Sea, Western Mediterranean (WM) (Martrat et al., 2014); c) Terrestrial TERR-alkanes curve, d) Alkenone SST curve and e) $ACL_{27\text{-}33}$ curve, from Core ND14Q-AR2, South Adriatic Sea (This study); f) TEX_{86} SST curve from Core GeoB 7702-3, Eastern Mediterranean (Castañeda et al., 2010); g) Composite $\delta^{18}O$ Asian Monsoon record, Central China (Cheng et al., 2016). Yellow shaded areas indicate HS1 interval as indicated by the various cited authors: a) **H1** (Voelker et al., 2009); b) **HS1a, b, c** (as indicated in Bazzicalupo *et al*., 2018); f) **HS1a, b** (Castaneda et al., 2016). Grey shaded area indicates the **HS1** division in the ND14Q-AR2 core (see text). Black Dashed line correlate HS1 divisions among climate records; grey dashed line is a tentative correlation between lowest monsoon activity registered in Asia (Cheng et al., 2016) and **HS1b** in our core (as indicated in the text).

6. Conclusions

In this work we present the first multiproxy record from the SAS that combines terrestrial and marine biomarkers with calcareous plankton assemblages in order to investigate centennial timescale climate variability during the last deglaciation. Alkenone SSTs, coccolithophore and planktonic foraminiferal assemblages along core ND14Q-AR2 evidence the influence of cold and fresher waters from melting continental alpine ice on the hydrology of the SAS that are consistent with Greenland ice core and SST reconstruction from other Mediterranean records. Terrestrial biomarkers suggest prevalent arid conditions on adjacent land and catchment basins interrupted by short humid phases accompanied by enhanced river run-off. Most importantly, our high-resolution reconstruction provides a detailed description of the HS1 (17-14.9 ka) that identifies a two-fold structure very similar to other records from the Mediterranean and other locations of the Northern Hemisphere. This feature is particularly expressed in the terrestrial proxy record highlighting the

role of atmospheric influence on the SAS, reflecting interactions with the cryosphere, e.g., ice melting from the Alps and delivery by the Po River. Shifts of the ITCZ associated to changes of the AMOC strength seems to be driving centennial scale changes during HS1, as further supported by the good correspondence of Mediterranean records with those of Central Asia indicating decreased monsoon activity. A brief event of Alpine and Apennine ice melting seems to have interrupted the humid/arid phases of HS1, highlighted by increased LE abundances. Finally, our results demonstrate that LE might be a valuable indicator of cold and low salinity waters from Alpine and Apennine glaciers melting and therefore a potential ecostratigraphical marker in the SAS during the deglaciation.

Acknowledgements

MISTRALS/ PALEOMEX program supported the biomarker analyses and P. Bazzicalupo stay at LOCEAN. Geoscience PhD scholarship - Università degli Studi di Bari to P. Bazzicalupo and Fondi Ateneo UNIBA 2018 to P. Maiorano funded coccolithophore analyses at DISTeGEO-UNIBA. This research has been also financially supported by ERC-Consolidator TIMED project (REP-683237), INGV Project 2019 (Paleoclimate variability during Late Holocene in the Central Mediterranean and Balkans: terrestrial and marine archive comparison). I. Cacho acknowledges support from the ICREA Academia programme from the Generalitat de Catalunya, J. Frigola from the Serra Húnter Programme (Generalitat de Catalunya).

Authors contributions

Pietro Bazzicalupo conceived the idea of the study with the support of Patrizia Maiorano and Marie-Alexandrine Sicre. Pietro Bazzicalupo carried out calcareous nannofossil analyses and interpretation with supervision of Patrizia Maiorano, and biomarker investigations and interpretation under the supervision of Marie-Alexandrine Sicre and Vincent Klein. Helena Checa carried out foraminiferal analysis and interpretation with supervision of Giulia Margaritelli and Leopoldo David Pena. Jamie Frigola carried out XRF core scanner analysis and interpretation. Pietro Bazzicalupo wrote the manuscript and developed the interpretative framework of the work with the support of Fabrizio Lirer, Patrizia Maiorano, Giulia Margaritelli and Marie-Alexandrine Sicre. Sergio Bonomo, Isabel Cacho, Antonio Cascella and Leopoldo David Pena provided critical revisions of the manuscript.

All the authors contributed to the discussions of the results.

References

Allen, J.R.M., Brandt, U., Brauer, A., Hubberten, H.-W., Huntley, B., Keller, J., Kraml, M., Mackensen, A., Mingram, J., Negendank, J.F.W., Nowaczyk, N.R., Oberhänsli, H., Watts, W.A., Wulf, S., Zolitschka, B., 1999. Rapid environmental changes in southern Europe during the last glacial period. Nature 400, 740–743. https://doi.org/10.1038/23432

Artegiani, A., Bregant, D., Paschini, E., Pinardi, N., Raicich, F., Russo, A., 1997. The adriatic sea general circulation. Part II: Baroclinic circulation structure. J. Phys. Oceanogr. 27, 1515–1532. https://doi.org/10.1175/1520-0485(1997)027<1515:TASGCP>2.0.CO;2

Arz, H.W., Pätzold, J., Müller, P.J., Moammar, M.O., Pätzgold, J., Müller, P.J., Moammar, M.O., 2003. Influence of Northern Hemisphere climate and global sea level rise on the restricted Red Sea marine environment during termination I.

Paleoceanography 18, 31-1–12.
Asioli, A., Trincardi, F., Lowe, J.J., Ariztegui, D., Langone, L., Oldfield, F., Old, F., Oldfield, F., 2001. Sub-millennial scale climatic oscillations in the central adriatic during the lateglacial: Palaeoceanographic implications. Quat. Sci. Rev. 20, 1201–1221. https://doi.org/10.1016/S0277-3791(00)00147-5
Asioli, A., Trincardi, F., Lowe, J.J., Oldfield, F., 1999. Short-term climate changes during the last glacial-holocene transition: Comparison between mediterranean records and the GRIP event stratigraphy. J. Quat. Sci. 14, 373–381. https://doi.org/10.1002/(SICI)1099-1417(199907)14:4<373::AID-JQS472>3.0.CO;2-T
Ausín, B., Flores, J.A., Sierro, F.J., Bárcena, M.A., Hernández-Almeida, I., Francés, G., Gutiérrez-Arnillas, E., Martrat, B., Grimalt, J.O., Cacho, I., 2015. Coccolithophore productivity and surface water dynamics in the Alboran Sea during the last 25 kyr. Palaeogeogr. Palaeoclimatol. Palaeoecol. 418, 126–140. https://doi.org/10.1016/j.palaeo.2014.11.011
Balestra, B., Marino, M., Monechi, S., Marano, C., Locaiono, F., 2008. Coccolithophore communities in the Gulf of Manfredonia (Southern Adriatic Sea): Data from water and surface sediments. Micropaleontology 54, 377–396.
Bard, E., Jouannic, C., Hamelin, B., Pirazzoli, P., Arnold, M., Faure, G., Sumosusastro, P., Syaefudin, 1996. Pleistocene sea levels and tectonic uplift based on dating of corals from Sumba Island, Indonesia. Geophys. Res. Lett. 23, 1473–1476. https://doi.org/10.1029/96GL01279
Bard, E., Rostek, F., Turon, J.L., Gendreau, S., 2000. Hydrological impact of Heinrich events in the subtropical Northeast Atlantic. Science (80-.). 289, 1321–1324. https://doi.org/10.1126/SCIENCE.289.5483.1321/SUPPL_FILE/1050685.XHTML
Bartolini, E., Claps, P., D'odorico, P., 2009. Interannual variability of winter precipitation in the European Alps: Relations with the North Atlantic Oscillation. Hydrol. Earth Syst. Sci. 13, 17–25. https://doi.org/10.5194/hess-13-17-2009
Baumann, K.-H., Boeckel, B., Frenz, M., 2004. Coccolith contribution to South Atlantic carbonate sedimentation; Coccolithophores; from molecular processes to global impact, in: Coccolithophores - From Molecular Processes to Global Impact. pp. 367–402. https://doi.org/10.1016/S0079-6352(99)80122-2
Bazzicalupo, P., Maiorano, P., Girone, A., Marino, M., Combourieu-Nebout, N., Incarbona, A., 2018. High-frequency climate fluctuations over the last deglaciation in the Alboran Sea, Western Mediterranean: Evidence from calcareous plankton assemblages. Palaeogeogr. Palaeoclimatol. Palaeoecol. 506, 226–241. https://doi.org/10.1016/j.palaeo.2018.06.042
Beaufort, L., De Garidel-Thoron, T., Mix, A.C., Pisias, N.G., 2001. ENSO-like forcing on oceanic primary production during the late pleistocene. Science (80-.). 293, 2440–2444. https://doi.org/10.1126/SCIENCE.293.5539.2440/ASSET/0954C48E-9D78-480C-B758-ED3C93AB33DA/ASSETS/GRAPHIC/SE3819804003.JPEG
Beaufort, L., Lancelot, Y., Camberlin, P., Cayre, O., Vincent, E., Bassinot, F., Labeyrie, L., 1997. Insolation cycles as a major control of equatorial Indian Ocean primary production. Science (80-.). 278, 1451–1454. https://doi.org/10.1126/science.278.5342.1451
Blaauw, M., Christen, J.A., 2011. Flexible paleoclimate age-depth models using an autoregressive gamma process. Bayesian Anal. 6, 457–474. https://doi.org/10.1214/11-BA618
Boeckel, B., Baumann, K.-H.H., 2004. Distribution of coccoliths in surface sediments of the south-eastern South Atlantic Ocean: Ecology, preservation and carbonate contribution. Mar. Micropaleontol. 51, 301–320. https://doi.org/10.1016/j.marmicro.2004.01.001
Bond, G., Heinrich, H., Broecker, W., Labeyrie, L., McManus, J., Andrews, J.T., Huon, S., Jantschik, R., Clasen, S., Simet, C., Tedesco, K., Klas, M., Bonani, G., Ivy, S., 1992. Evidence for massive discharges of icebers into the North Atlantic ocean during the last glacial period. Nature 359, 710–713.
Bonomo, S., Cascella, A., Alberico, I., Ferraro, L., Giordano, L., Lirer, F., Vallefuoco, M., Marsella, E., 2014. Coccolithophores from near the Volturno estuary (central Tyrrhenian Sea). Mar. Micropaleontol. 111, 26–37. https://doi.org/10.1016/j.marmicro.2014.06.001
Bonomo, S., Cascella, A., Alberico, I., Sorgato, S., Pelosi, N., Ferraro, L., Lirer, F., Vallefuoco, M., Bellucci, L., Agnini, C., Pappone, G., 2016. Reworked Coccoliths as runoff proxy for the last 400 years: The case of Gaeta Gulf (central Tyrrhenian Sea, Central Italy). Palaeogeogr. Palaeoclimatol. Palaeoecol. 459, 15–28. https://doi.org/10.1016/j.palaeo.2016.06.037
Broecker, W., Bond, G., Klas, M., Clark, E., Mcmanus, J., 1992. Origin of the northern Atlantic's Heinrich events. Clim. Dyn. 6,

265–273. https://doi.org/10.1007/BF00193540

Cacho, I., Grimalt, J.O., Canals, M., Sbaffi, L., Shackleton, N.J., Schönfeld, J., Zahn, R., 2001. Variability of the western Mediterranean Sea surface temperature during the last 25,000 years and its connection with the Northern Hemisphere climatic change. Paleoceanography 16, 40–52. https://doi.org/10.1029/SP010

Cacho, I., Grimalt, J.O., Pelejero, C., Canals, M., Sierro, F.J., Flores, J.A., Shackleton, N.J., 1999. Dansgaard-Oeschger and Heinrich event imprints in Alboran Sea paleotemperatures. Paleoceanography 14, 698–705. https://doi.org/10.1029/1999PA900044

Cacho, I., Grimalt, J.O., Sierro, F.J., Shackleton, N., Canals, M., 2000. Evidence for enhanced Mediterranean thermohaline circulation during rapid climatic coolings. Earth Planet. Sci. Lett. 183, 417–429. https://doi.org/10.1016/S0012-821X(00)00296-X

Capotondi, L., Girone, A., Lirer, F., Bergami, C., Verducci, M., Vallefuoco, M., Afferri, A., Ferraro, L., Pelosi, N., De Lange, G.J., 2016. Central Mediterranean Mid-Pleistocene paleoclimatic variability and its association with global climate. Palaeogeogr. Palaeoclimatol. Palaeoecol. 442, 72–83. https://doi.org/10.1016/j.palaeo.2015.11.009

Capotondi, L., Maria Borsetti, A., Morigi, C., Borsetti, A.M., Morigi, C., 1999. Foraminiferal ecozones, a high resolution proxy for the late Quaternary biochronology in the central Mediterranean Sea. Mar. Geol. 153, 253–274. https://doi.org/10.1016/S0025-3227(98)00079-6

Capotondi, L., Soroldoni, E., Principato, M.S., Corselli, C., Sezione, I.C.N.R., Bologna, M., 2004. Late Quaternary planktonic foraminiferal distributions : problems related to size fraction. Proc. First Ital. Meet. Environ. Micropaleontol. 1–6.

Cascella, A., Bonomo, S., Jalali, B., Sicre, M.-A., Pelosi, N., Schmidt, S., Lirer, F., 2019. Climate variability of the last 2700 years in the Southern Adriatic Sea: Coccolithophore evidences, The Holocene.

Castañeda, I.S., Schefuß, E., Pätzold, J., Sinninghe Damsté, J.S., Weldeab, S., Schouten, S., 2010. Millennial-scale sea surface temperature changes in the eastern Mediterranean (Nile River Delta region) over the last 27,000 years. Paleoceanography 25, 1–13. https://doi.org/10.1029/2009PA001740

Castañeda, I.S., Schouten, S., Pätzold, J., Lucassen, F., Kasemann, S., Kuhlmann, H., Schefuß, E., 2016. Hydroclimate variability in the Nile River Basin during the past 28,000 years. Earth Planet. Sci. Lett. 438, 47–56. https://doi.org/10.1016/j.epsl.2015.12.014

Cheng, H., Edwards, R.L., Sinha, A., Spötl, C., Yi, L., Chen, S., Kelly, M., Kathayat, G., Wang, X., Li, X., Kong, X., Wang, Y., Ning, Y., Zhang, H., 2016. The Asian monsoon over the past 640,000 years and ice age terminations. Nature 534, 640–646. https://doi.org/10.1038/nature18591

Cita, M.B., Vergnaud-Grazzini, C., Robert, C., Chamley, H., Ciaranfi, N., d'Onofrio, S., 1977. Paleoclimatic Record of a Long Deep Sea Core from the Eastern Mediterranean. Quat. Res. 8, 205–235. https://doi.org/10.1016/0033-5894(77)90046-1

Clark, P.U., Shakun, J.D., Baker, A., Bartlein, P.J., Brewer, S., Brook, E., Carlson, A.E., Cheng, H., Kaufman, D.S., Liu, Z., Marchitto, T.M., Mix, A.C., Morrill, C., Otto-Bliesner, B.L., Pahnke, K., Russell, J.M., Whitlock, C., Adkins, J.F., Blois, J.L., Clark, J., Colman, S.M., Curry, W.B., Flower, B.P., He, F., Johnson, T.C., Lynch-Stieglitz, J., Markgraf, V., McManus, J., Mitrovica, J.X., Moreno, P.I., Williams, J.W., 2012. Global climate evolution during the last deglaciation. Proc. Natl. Acad. Sci. 109, E1134–E1142. https://doi.org/10.1073/pnas.1116619109

Colmenero-Hidalgo, E., Flores, J.A., Sierro, F.J., 2002. Biometry of Emiliania huxleyi and its biostratigraphic significance in the Eastern North Atlantic Ocean and Western Mediterranean Sea in the last 20 000 years. Mar. Micropaleontol. 46, 247–263. https://doi.org/10.1016/S0377-8398(02)00065-8

Colmenero-Hidalgo, E., Flores, J.A., Sierro, F.J., Bárcena, M.Á., Löwemark, L., Schönfeld, J., Grimalt, J.O., 2004. Ocean surface water response to short-term climate changes revealed by coccolithophores from the Gulf of Cadiz (NE Atlantic) and Alboran Sea (W Mediterranean). Palaeogeogr. Palaeoclimatol. Palaeoecol. 205, 317–336. https://doi.org/10.1016/j.palaeo.2003.12.014

Combourieu-Nebout, N., Paterne, M., Turon, J.-L., Siani, G., Paterne-, M., Turon, J.-L., Siani-, G., Paterne, M., Turon, J.-L., Siani, G., 1998. a High-Resolution Record of the Last Deglaciation in the Central Mediterranean Sea. Quat. Sci. Rev. 17, 303–317.

Combourieu Nebout, N., Peyron, O., Dormoy, I., Desprat, S., Beaudouin, C., Kotthoff, U., Marret, F., 2009. Rapid climatic variability in the west Mediterranean during the last 25000 years from high resolution pollen data. Clim. Past 5, 503–521.

Conte, M.H., Sicre, M.-A., Rühlemann, C., Weber, J.C., Schulte, S., Schulz-Bull, D., Blanz, T., 2006. Global temperature calibration

of the alkenone unsaturation index ($U^{K'}_{37}$) in surface waters and comparison with surface sediments. Geochemistry, Geophys. Geosystems 7, n/a-n/a. https://doi.org/10.1029/2005GC001054

Correggiari, A., Field, M.E., Trincardi, F., 1996. Late Quaternary transgressive large dunes on the sediment-starved Adriatic shelf. Geol. Soc. London, Spec. Publ. 117, 155–169. https://doi.org/10.1144/GSL.SP.1996.117.01.09

Corselli, C., Principato, M.S., Maffioli, P., Crudeli, D., 2002. Changes in planktonic assemblages during sapropel S5 deposition: Evidence from Urania Basin area, eastern Mediterranean. Paleoceanography 17, 1-1–30. https://doi.org/10.1029/2000pa000536

Dansgaard, W., Johnsen, S.J., Clausen, H.B., Dahl-Jensen, D., Gundestrup, N.S., Hammer, C.U., Hvidberg, C.S., Steffensen, J.P., Sveinbjörnsdottir, A.E., Jouzel, J., Bond, G., 1993. Evidence for general instability of past climate from a 250-kyr ice-core record. Nature 364, 218–220. https://doi.org/10.1038/364218a0

De Castro Coppa, M.G., Moncharmont Zei, M., Placella., B., Sgarella, F., Taddei Ruggiero, E., 1980. Distribuzione stagionale e verticale dei Foraminiferi planctonici del Golfo di Napoli. Boll. Soc. Nat. Napoli 1–25.

Deplazes, G., Lückge, A., Peterson, L.C., Timmermann, A., Hamann, Y., Hughen, K.A., Röhl, U., Laj, C., Cane, M.A., Sigman, D.M., Haug, G.H., 2013. Links between tropical rainfall and North Atlantic climate during the last glacial period. Nat. Geosci. 6, 213–217. https://doi.org/10.1038/ngeo1712

Desprat, S., Combourieu-Nebout, N., Essallami, L., Sicre, M.-A.A., Dormoy, I., Peyron, O., Siani, G., Bout Roumazeilles, V., Turon, J.L., Bout-Roumazeilles, V., Turon, J.L., 2013. Deglacial and holocene vegetation and climatic changes in the southern central Mediterranean from a direct land-sea correlation. Clim. Past 9, 767–787. https://doi.org/10.5194/cp-9-767-2013

Di Stefano, A., Foresi, L.M., Incarbona, A., Sprovieri, M., Vallefuoco, M., Iorio, M., Pelosi, N., Di Stefano, E., Sangiorgi, P., Budillon, F., 2015. Mediterranean coccolith ecobiostratigraphy since the penultimate Glacial (the last 145,000years) and ecobioevent traceability. Mar. Micropaleontol. 115, 24–38. https://doi.org/10.1016/j.marmicro.2014.12.002

Di Stefano, E., Incarbona, A., 2004. High-resolution palaeoenvironmental reconstruction of ODP Hole 963D (Sicily Channel) during the last deglaciation based on calcareous nannofossils. Mar. Micropaleontol. 52, 241–254. https://doi.org/10.1016/j.marmicro.2004.04.009

Eglinton, T.I., Eglinton, G., 2008. Molecular proxies for paleoclimatology. Earth Planet. Sci. Lett. 275, 1–16. https://doi.org/10.1016/j.epsl.2008.07.012

Essallami, L., Sicre, M.-A., Kallel, N., Labeyrie, L., Siani, G., 2007. Hydrological changes in the Mediterranean Sea over the last 30,000 years. Geochemistry, Geophys. Geosystems 8. https://doi.org/10.1029/2007GC001587

Fairbanks, R.G., Mortlock, R.A., Chiu, T.C., Cao, L., Kaplan, A., Guilderson, T.P., Fairbanks, T.W., Bloom, A.L., Grootes, P.M., Nadeau, M.J., 2005. Radiocarbon calibration curve spanning 0 to 50,000 years BP based on paired 230Th/234U/238U and 14C dates on pristine corals. Quat. Sci. Rev. 24, 1781–1796. https://doi.org/10.1016/j.quascirev.2005.04.007

Favaretto, S., Asioli, A., Miola, A., Piva, A., 2008. Preboreal climatic oscillations recorded by pollen and foraminifera in the southern Adriatic Sea. Quat. Int. 190, 89–102. https://doi.org/10.1016/j.quaint.2008.04.005

Fletcher, W.J., Sánchez Goñi, M.F., 2008. Orbital- and sub-orbital-scale climate impacts on vegetation of the western Mediterranean basin over the last 48,000 yr. Quat. Res. 70, 451–464. https://doi.org/10.1016/j.yqres.2008.07.002

Fletcher, W.J., Sánchez Goñi, M.F., Allen, J.R.M., Cheddadi, R., Combourieu-Nebout, N., Huntley, B., Lawson, I., Londeix, L., Magri, D., Margari, V., Müller, U.C., Naughton, F., Novenko, E., Roucoux, K., Tzedakis, P.C., 2010. Millennial-scale variability during the last glacial in vegetation records from Europe. Quat. Sci. Rev. 29, 2839–2864. https://doi.org/10.1016/j.quascirev.2009.11.015

Flores, J.A., Colmenero-Hidalgo, E., Mejía-Molina, A.E., Baumann, K.H., Henderiks, J., Larsson, K., Prabhu, C.N., Sierro, F.J., Rodrigues, T., 2010. Distribution of large Emiliania huxleyi in the Central and Northeast Atlantic as a tracer of surface ocean dynamics during the last 25,000years. Mar. Micropaleontol. 76, 53–66. https://doi.org/10.1016/j.marmicro.2010.05.001

Flores, J.A., Gersonde, R.R., Sierro, F.J., Niebler, H.-S., 2000. Southern ocean pleistocene calcareous nannofossil events: Calibration with isotope and geomagnetic stratigraphies. Mar. Micropaleontol. 40, 377–402. https://doi.org/10.1016/S0377-8398(00)00047-5

Flores, J.A., Sierro, F.J., 1997. Revised technique for calculation of calcareous nannofossil accumulation rates. Micropaleontology

43, 321–324. https://doi.org/10.2307/1485832
Flores, J.A., Sierro, F.J., Francés, G., Vázquez, A., Zamarreno, I., 1997. The last 100,000 years in the western Mediterranean: Sea surface water and frontal dynamics as revealed by coccolithophores. Mar. Micropaleontol. 29, 351–366. https://doi.org/10.1016/S0377-8398(96)00029-1
Frigola, J., Moreno, A., Cacho, I., Canals, M., Sierro, F.J., Flores, J.A., Grimalt, J.O., 2008. Evidence of abrupt changes in Western Mediterranean Deep Water circulation during the last 50 kyr: A high-resolution marine record from the Balearic Sea. Quat. Int. 181, 88–104. https://doi.org/10.1016/j.quaint.2007.06.016
Gačić, M., Civitarese, G., Miserocchi, S., Cardin, V., Crise, A., Mauri, E., 2002. The open-ocean convection in the Southern Adriatic: A controlling mechanism of the spring phytoplankton bloom. Cont. Shelf Res. 22, 1897–1908. https://doi.org/10.1016/S0278-4343(02)00050-X
Gačić, M., Marullo, S., Santoleri, R., Bergamasco, A., 1997. Analysis of the seasonal and interannual variability of the sea surface temperature field in the Adriatic Sea from AVHRR data (1984-1992). J. Geophys. Res. Ocean. 102, 22937–22946. https://doi.org/10.1029/97JC01720
Gagosian, R.B., Peltzer, E.T., 1986. The importance of atmospheric input of terrestrial organic material to deep sea sediments. Org. Geochem. 10, 661–669. https://doi.org/10.1016/S0146-6380(86)80002-X
Geraga, M., Mylona, G., Tsaila-Monopoli, S., Papatheodorou, G., Ferentinos, G., 2008. Northeastern Ionian Sea: Palaeoceanographic variability over the last 22 ka. J. Mar. Syst. 74, 623–638. https://doi.org/10.1016/J.JMARSYS.2008.05.019
Giunta, S., Negri, A., Morigi, C., Capotondi, L., Combourieu-Nebout, N., Emeis, K.C.K., Sangiorgi, F., Vigliotti, L., 2003. Coccolithophorid ecostratigraphy and multi-proxy paleoceanographic reconstruction in the Southern Adriatic Sea during the last deglacial time (Core AD91-17). Palaeogeogr. Palaeoclimatol. Palaeoecol. 190, 39–59. https://doi.org/10.1016/S0031-0182(02)00598-9
Hagino, K., Okada, H., Matsuoka, H., 2005. Coccolithophore assemblages and morphotypes of Emiliania huxleyi in the boundary zone between the cold Oyashio and warm Kuroshio currents off the coast of Japan. Mar. Micropaleontol. 55, 19–47. https://doi.org/10.1016/j.marmicro.2005.02.002
Hemleben, C., Spindler, M., Anderson, O.R., 1989. Taxonomy and Species Features, in: Modern Planktonic Foraminifera. Springer New York, New York, NY, pp. 8–32. https://doi.org/10.1007/978-1-4612-3544-6_2
Hodell, D.A., Nicholl, J.A., Bontognali, T.R.R., Danino, S., Dorador, J., Dowdeswell, J.A., Einsle, J., Kuhlmann, H., Martrat, B., Mleneck-Vautravers, M.J., Rodríguez-Tovar, F.J., Röhl, U., 2017. Anatomy of Heinrich Layer 1 and its role in the last deglaciation. Paleoceanography 32, 284–303. https://doi.org/10.1002/2016PA003028
Huang, J., Wan, S., Li, A., Li, T., 2019. Two-phase structure of tropical hydroclimate during Heinrich Stadial 1 and its global implications. Quat. Sci. Rev. 222, 105900. https://doi.org/10.1016/j.quascirev.2019.105900
Jalali, B., Sicre, M.-A., Bassetti, M.A., Kallel, N., 2016. Holocene climate variability in the North-Western Mediterranean Sea (Gulf of Lions). Clim. Past 12, 91–101. https://doi.org/10.5194/cp-12-91-2016
Jalali, B., Sicre, M.-A., Kallel, N., Azuara, J., Combourieu-Nebout, N., Bassetti, M.A., Klein, V., 2017. High-resolution Holocene climate and hydrological variability from two major Mediterranean deltas (Nile and Rhone). Holocene 27, 1158–1168. https://doi.org/10.1177/0959683616683258
Jalali, B., Sicre, M.-A., Klein, V., Schmidt, S., Maselli, V., Lirer, F., Bassetti, M.A., Toucanne, S., Jorry, S.J., Insinga, D.D., Petrosino, P., Châles, F., 2018. Deltaic and Coastal Sediments as Recorders of Mediterranean Regional Climate and Human Impact Over the Past Three Millennia. Paleoceanogr. Paleoclimatology 33, 579–593. https://doi.org/10.1029/2017PA003298
Jiménez-Amat, P., Zahn, R., 2015. Offset timing of climate oscillations during the last two glacial-interglacial transitions connected with large-scale freshwater perturbation. Paleoceanography 30, 768–788. https://doi.org/10.1002/2014PA002710
Jonkers, L., Brummer, G.J.A., Peeters, F.J.C., Van Aken, H.M., De Jong, M.F., 2010. Seasonal stratification, shell flux, and oxygen isotope dynamics of leftcoiling N. pachyderma and T. quinqueloba in the western subpolar North Atlantic. Paleoceanography 25, 1–13. https://doi.org/10.1029/2009PA001849
Jordan, R.W., Cros, L., Young, J.R., 2004. A revised classification scheme for living haptophytes. Micropaleontology 50, 55–79. https://doi.org/10.2113/50.Suppl_1.55

Kageyama, M., Mignot, J., Swingedouw, D., Marzin, C., Alkama, R., Marti, O., 2009. Glacial climate sensitivity to different states of the atlantic meridional overturning circulation: Results from the IPSL model. Clim. Past 5, 551–570. https://doi.org/10.5194/cp-5-551-2009

Kotthoff, U., Koutsodendris, A., Pross, J., Schmiedl, G., Bornemann, A., Kaul, C., Marino, G., Peyron, O., Schiebel, R., 2011. Impact of Lateglacial cold events on the northern Aegean region reconstructed from marine and terrestrial proxy data. J. Quat. Sci. 26, 86–96. https://doi.org/10.1002/jqs.1430

Kwiecien, O., Arz, H.W., Lamy, F., Plessen, B., Bahr, A., Haug, G.H., 2009. North Atlantic control on precipitation pattern in the eastern Mediterranean/Black Sea region during the last glacial. Quat. Res. 71, 375–384. https://doi.org/10.1016/j.yqres.2008.12.004

Lascaratos, A., 1993. Estimation of deep and intermediate water mass formation rates in the Mediterranean Sea. Deep Sea Res. Part II Top. Stud. Oceanogr. 40, 1327–1332. https://doi.org/10.1016/0967-0645(93)90072-U

Laskar, J., Robutel, P., Joutel, F., Gastineau, M., Correia, A.C.M., Levrard, B., 2004. A long-term numerical solution for the insolation quantities of the Earth. Astron. Astrophys. 428, 261–285. https://doi.org/10.1051/0004-6361:20041335

Lipizer, M., Partescano, E., Rabitti, A., Giorgetti, A., Crise, A., 2014. Qualified temperature, salinity and dissolved oxygen climatologies in a changing Adriatic Sea. Ocean Sci. 10, 771–797. https://doi.org/10.5194/os-10-771-2014

Liu, J.P.P., Milliman, J.D., 2004. Reconsidering melt-water pulses 1A and 1B: Global impacts of rapid sea-level rise. J. Ocean Univ. China 3, 183–190. https://doi.org/10.1007/s11802-004-0033-8

Lowe, J.J., Blockley, S.P., Trincardi, F., Asioli, A., Cattaneo, A., Matthews, I.P., Pollard, M., Wulf, S., 2007. Age modelling of late Quaternary marine sequences in the Adriatic: Towards improved precision and accuracy using volcanic event stratigraphy. Cont. Shelf Res. 27, 560–582. https://doi.org/10.1016/j.csr.2005.12.017

Magri, D., Sadori, L., 1999. Late Pleistocene and Holocene pollen stratigraphy at Lago di Vico, central Italy. Veg. Hist. Archaeobot. 8, 247–260. https://doi.org/10.1007/BF01291777

Maiorano, P., Girone, A., Marino, M., Kucera, M., Pelosi, N., 2016. Sea surface water variability during the Mid-Brunhes inferred from calcareous plankton in the western Mediterranean (ODP Site 975). Palaeogeogr. Palaeoclimatol. Palaeoecol. 459, 229–248. https://doi.org/10.1016/j.palaeo.2016.07.006

Manca, B.B., Kovaĉević, V., Gaĉić, M., Viezzoli, D., 2002. Dense water formation in the Southern Adriatic Sea and spreading into the Ionian Sea in the period 1997–1999. J. Mar. Syst. 33–34, 133–154. https://doi.org/10.1016/S0924-7963(02)00056-8

Margaritelli, G., Cisneros, M., Cacho, I., Capotondi, L., Vallefuoco, M., Rettori, R., Lirer, F., 2018. Climatic variability over the last 3000 years in the central - western Mediterranean Sea (Menorca Basin) detected by planktonic foraminifera and stable isotope records. Glob. Planet. Change 169, 179–187. https://doi.org/10.1016/j.gloplacha.2018.07.012

Margaritelli, G., Lirer, F., Schroeder, K., Alberico, I., Dentici, M.P., Caruso, A., 2020. Globorotalia truncatulinoides in Central - Western Mediterranean Sea during the Little Ice Age. Mar. Micropaleontol. 161, 101921. https://doi.org/10.1016/J.MARMICRO.2020.101921

Martinez-Ruiz, F., Kastner, M., Gallego-Torres, D., Rodrigo-Gámiz, M., Nieto-Moreno, V., Ortega-Huertas, M., 2015. Paleoclimate and paleoceanography over the past 20,000yr in the Mediterranean Sea Basins as indicated by sediment elemental proxies. Quat. Sci. Rev. 107, 25–46. https://doi.org/10.1016/j.quascirev.2014.09.018

Martrat, B., Grimalt, J.O., Lopez-Martinez, C., Cacho, I., Sierro, F.J., Flores, J.A., Zahn, R., Canals, M., Curtis, J.H., Hodell, D.A., 2004. Abrupt temperature changes in the Western Mediterranean over the past 250,000 years. Science (80-.). 306, 1762–1765. https://doi.org/10.1126/science.1101706

Martrat, B., Jimenez-Amat, P., Zahn, R., Grimalt, J.O., 2014. Similarities and dissimilarities between the last two deglaciations and interglaciations in the North Atlantic region. Quat. Sci. Rev. 99, 122–134. https://doi.org/10.1016/j.quascirev.2014.06.016

Mcmanus, J.F., Francois, R., Gherardi, J.-M., Keigwin, L.D., Brown-Leger, S., 2004. Collapse and rapid resumption of Atlantic meridional circulation linked to deglacial climate changes. Nature 428, 834–837. https://doi.org/10.1038/nature02494

Melki, T., 2011. Variation of deepwater convection in the western Mediterranean Sea (Gulf of Lion) during the last 28 ka. Quat. Int. 241, 160–168. https://doi.org/10.1016/j.quaint.2011.04.001

Melki, T., Kallel, N., Jorissen, F.J., Guichard, F., Dennielou, B., Berné, S., Labeyrie, L., Fontugne, M., 2009. Abrupt climate change,

sea surface salinity and paleoproductivity in the western Mediterranean Sea (Gulf of Lion) during the last 28 kyr. Palaeogeogr. Palaeoclimatol. Palaeoecol. 279, 96–113. https://doi.org/10.1016/j.palaeo.2009.05.005

Molfino, B., Mcintyre, A., 1990. Precessional forcing of nutricline dynamics in the equatorial Atlantic. Science (80-.). 249, 766–769. https://doi.org/10.1126/science.249.4970.766

Moreno, A., Cacho, I., Canals, M., Grimalt, J.O., Sánchez-Goñi, M.F., Shackleton, N., Sierro, F.J., 2005. Links between marine and atmospheric processes oscillating on a millennial time-scale. A multi-proxy study of the last 50,000 yr from the Alboran Sea (Western Mediterranean Sea). Quat. Sci. Rev. 24, 1623–1636. https://doi.org/10.1016/j.quascirev.2004.06.018

Narciso, Á., Flores, J.A., Cachao, M., Piva, A., Asioli, A., Andersen, N., Schneider, R., 2012. Late Glacial-Holocene transition in the southern Adriatic Sea: Coccolithophore and Foraminiferal evidence. Micropaleontology 58, 523–538.

Naughton, F., Sánchez Goñi, M.F., Kageyama, M., Bard, E., Duprat, J., Cortijo, E., Desprat, S., Malaizé, B., Joly, C., Rostek, F., Turon, J.L., 2009. Wet to dry climatic trend in north-western Iberia within Heinrich events. Earth Planet. Sci. Lett. 284, 329–342. https://doi.org/10.1016/j.epsl.2009.05.001

Naughton, F., Sanchez Goñi, M.F., Rodrigues, T., Salgueiro, E., Costas, S., Desprat, S., Duprat, J., Michel, E., Rossignol, L., Zaragosi, S., Voelker, A.H.L., Abrantes, F.F., 2016. Climate variability across the last deglaciation in NW Iberia and its margin. Quat. Int. 414, 9–22. https://doi.org/10.1016/j.quaint.2015.08.073

NGRIP, (North Greenland Ice Core Project members), 2004. High-resolution record of Northern Hemisphere climate extending into the last interglacial period. Nature 431, 147–151. https://doi.org/10.1038/nature02805

Nieto-Moreno, V., Martínez-Ruiz, F., Giralt, S., Jiménez-Espejo, F., Gallego-Torres, D., Rodrigo-Gámiz, M., García-Orellana, J., Ortega-Huertas, M., De Lange, G.J., 2011. Tracking climate variability in the western Mediterranean during the Late Holocene: A multiproxy approach. Clim. Past 7, 1395–1414. https://doi.org/10.5194/cp-7-1395-2011

Orlić, M., Gačić, M., LaViolette, P.E., 1992. The currents and circulation of the Adriatic Sea. Oceanol. Acta 15, 109–124.

Ortiz, J.D., Mix, A.C., Rugh, W., Watkins, J.M., Collier, R.W., 1996. Deep-dwelling planktonic foraminifera of the northeastern Pacific Ocean reveal environmental control of oxygen and carbon isotopic disequilibria. Geochim. Cosmochim. Acta 60, 4509–4523. https://doi.org/10.1016/S0016-7037(96)00256-6

Paasche, E., 2002. A review of the coccolithophorid Emiliania huxleyi (Prymnesiophyceae), with particular reference to growth, coccolith formation, and calcification-photosynthesis interactions E. Phycologia 40, 503–529.

Pérez-Folgado, M., Sierro, F.J., Flores, J.A., Cacho, I., Grimalt, J.O., Zahn, R., Shackleton, N.J., 2003. Western Mediterranean planktonic foraminifera events and millennial climatic variability during the last 70 kyr. Mar. Micropaleontol. 48, 49–70. https://doi.org/10.1016/S0377-8398(02)00160-3

Pinardi, N., Masetti, E., 2000. Variability of the large scale general circulation of the Mediterranean Sea from observations and modelling: A review. Palaeogeogr. Palaeoclimatol. Palaeoecol. 158, 153–173. https://doi.org/10.1016/S0031-0182(00)00048-1

Piva, A., Asioli, A., Trincardi, F., Schneider, R.R., Vigliotti, L., 2008. Late-Holocene climate variability in the Adriatic Sea (Central Mediterranean). Holocene 18, 153–167. https://doi.org/10.1177/0959683607085606

Principato, M.S., Crudeli, D., Ziveri, P., Slomp, C.P., Corselli, C., Erba, E., de Lange, G.J., 2006. Phyto_ and zooplankton paleofluxes during the deposition of sapropel S1 (eastern Mediterranean): Biogenic carbonate preservation and paleoecological implications. Palaeogeogr. Palaeoclimatol. Palaeoecol. 235, 8–27. https://doi.org/10.1016/j.palaeo.2005.09.021

Pujol, C., Vergnaud-Grazzini, C., 1995. Distribution patterns of live planktic foraminifers as related to regional hydrography and productive systems of the Mediterranean Sea. Mar. Micropaleontol. 25, 187–217. https://doi.org/10.1016/0377-8398(95)00002-I

Rahmstorf, S., 1994. Rapid climate transitions in a coupled ocean–atmosphere model. Nature 372, 82–85. https://doi.org/10.1038/372082a0

Rasmussen, S.O., Andersen, K.K., Svensson, A.M., Steffensen, J.P., Vinther, B.M., Clausen, H.B., Siggaard-Andersen, M.L., Johnsen, S.J., Larsen, L.B., Dahl-Jensen, D., Bigler, M., Röthlisberger, R., Fischer, H., Goto-Azuma, K., Hansson, M.E., Ruth, U., 2006. A new Greenland ice core chronology for the last glacial termination. J. Geophys. Res. Atmos. 111, 1–16. https://doi.org/10.1029/2005JD006079

Rasmussen, S.O., Bigler, M., Blockley, S.P., Blunier, T., Buchardt, S.L., Clausen, H.B., Cvijanovic, I., Dahl-Jensen, D., Johnsen, S.J., Fischer, H., Gkinis, V., Guillevic, M., Hoek, W.Z., Lowe, J.J., Pedro, J.B., Popp, T., Seierstad, I.K., Steffensen, J.P., Svensson, A.M., Vallelonga, P., Vinther, B.M., Walker, M.J.C., Wheatley, J.J., Winstrup, M., 2014. A stratigraphic framework for abrupt climatic changes during the Last Glacial period based on three synchronized Greenland ice-core records: Refining and extending the INTIMATE event stratigraphy. Quat. Sci. Rev. 106, 14–28. https://doi.org/10.1016/j.quascirev.2014.09.007

Repschläger, J., Weinelt, M., Kinkel, H., Andersen, N., Garbe-Schönberg, D., Schwab, C., 2015. Response of the subtropical North Atlantic surface hydrography on deglacial and Holocene AMOC changes. Paleoceanography 30, 456–476. https://doi.org/10.1002/2014PA002637

Ridente, D., Trincardi, F., 2006. Active foreland deformation evidenced by shallow folds and faults affecting late Quaternary shelf-slope deposits (Adriatic Sea, Italy). Basin Res. 18, 171–188. https://doi.org/10.1111/j.1365-2117.2006.00289.x

Ridente, D., Trincardi, F., 2002. Eustatic and tectonic control on deposition and lateral variability of quaternary regressive sequences in the Adriatic basin (Italy). Mar. Geol. 184, 273–293. https://doi.org/10.1016/S0025-3227(01)00296-1

Rigual-Hernández, A.S., Sierro, F.J., Bárcena, M.A., Flores, J.A., Heussner, S., 2012. Seasonal and interannual changes of planktic foraminiferal fluxes in the Gulf of Lions (NW Mediterranean) and their implications for paleoceanographic studies: Two 12-year sediment trap records. Deep. Res. Part I Oceanogr. Res. Pap. 66, 26–40. https://doi.org/10.1016/j.dsr.2012.03.011

Rodrigo-Gámiz, M., Martínez-Ruiz, F., Jiménez-Espejo, F.J., Gallego-Torres, D., Nieto-Moreno, V., Romero, O., Ariztegui, D., 2011. Impact of climate variability in the western Mediterranean during the last 20,000 years: Oceanic and atmospheric responses. Quat. Sci. Rev. 30, 2018–2034. https://doi.org/10.1016/j.quascirev.2011.05.011

Rogerson, M., Colmenero-Hidalgo, E., Levine, R.C., Rohling, E.J., Voelker, A.H.L., Bigg, G.R., Schönfeld, J., Cacho, I., Sierro, F.J., Löwemark, L., Reguera, M.I., de Abreu, L., Garrick, K., 2010. Enhanced Mediterranean-Atlantic exchange during Atlantic freshening phases. Geochemistry, Geophys. Geosystems 11, 1–22. https://doi.org/10.1029/2009GC002931

Rohling, E.J., Hayes, A., De Rijk, S., Kroon, D., Zachariasse, W.J., Eisma, D., 1998. Abrupt cold spells in the northwest Mediterranean. Paleoceanography 13, 316–322. https://doi.org/10.1029/98PA00671

Rohling, E.J., Jorissen, F.J., De Stiger, H.C., 1997. 200 Year interruption of Holocene sapropel formation in the Adriatic Sea. J. Micropalaeontology 16, 97–108. https://doi.org/10.1144/jm.16.2.97

Rohling, E.J., Jorissen, F.J., Grazzini, C.V., Zachariasse, W.J., 1993. Northern Levantine and Adriatic Quaternary planktic foraminifera; Reconstruction of paleoenvironmental gradients. Mar. Micropaleontol. 21, 191–218. https://doi.org/10.1016/0377-8398(93)90015-P

Sanchez Goñi, M.F., Cacho, I., Turon, J.L., Guiot, J., Sierro, F.J., Peypouquet, J.P., Grimalt, J.O., Shackleton, N.J., 2002. Synchroneity between marine and terrestrial responses to millennial scale climatic variability during the last glacial period in the Mediterranean region. Clim. Dyn. 19, 95–105. https://doi.org/10.1007/s00382-001-0212-x

Sangiorgi, F., Capotondi, L., Combourieu Nebout, N., Vigliotti, L., Brinkhuis, H., Giunta, S., Lotter, A.F., Morigi, C., Negri, A., Reichart, G.J., 2003. Holocene seasonal sea-surface temperature variations in the southern Adriatic Sea inferred from a multiproxy approach. J. Quat. Sci. 18, 723–732. https://doi.org/10.1002/jqs.782

Sanvoisin, R., D'Onofrio, S., Lucchi, R., Violanti, D., Castradori, D., 1993. 1 Ma paleoclimatic record from the Eastern Mediterranean - Marflux project: First results of a micropaleontological and sedimentological investigation of a long piston core from the Calabrian Ridge. Alp. Mediterr. Quat. 6, 169–187.

Schiebel, R., Bijma, J., Hemleben, C., 1997. Population dynamics of the planktic foraminifer Globigerina hulloides from the eastern North Atlantic. Deep. Res. Part I Oceanogr. Res. Pap. 44, 1701–1713. https://doi.org/10.1016/S0967-0637(97)00036-8

Schiebel, R., Schmuker, B., Alves, M., Hemleben, C., 2002. Tracking the Recent and late Pleistocene Azores front by the distribution of planktic foraminifers. J. Mar. Syst. 37.

Schiebel, R., Waniek, J., Bork, M., Hemleben, C., 2001. Planktic foraminiferal production stimulated by chlorophyll redistribution and entrainment of nutrients. Deep. Res. Part I Oceanogr. Res. Pap. 48, 721–740. https://doi.org/10.1016/S0967-0637(00)00065-0

Schirrmacher, J., Weinelt, M., Blanz, T., Andersen, N., Salgueiro, E., Schneider, R.R., 2019. Multi-decadal climate variability in

891 southern Iberia during the mid- to late-Holocene. Clim. Past Discuss. 1–29. https://doi.org/10.5194/cp-2018-158
892 Schmidt, D.N., Thierstein, H.R., Bollmann, J., Schiebel, R., 2004. Abiotic Forcing of Plankton Evolution in the Cenozoic. Science
893 (80-.). 303, 207–210. https://doi.org/10.1126/science.1090592
894 Schwab, C., Kinkel, H., Weinelt, M., Repschlger, J., 2012. Coccolithophore paleoproductivity and ecology response to deglacial and
895 Holocene changes in the Azores Current System. Paleoceanography 27, 1–18. https://doi.org/10.1029/2012PA002281
896 Seidov, D., Maslin, M., 1999. North Atlantic deep water circulation collapse during Heinrich events. Geology 27, 23.
897 https://doi.org/10.1130/0091-7613(1999)027<0023:NADWCC>2.3.CO;2
898 Siani, G., Magny, M., Paterne, M., Debret, M., Fontugne, M., 2013. Paleohydrology reconstruction and Holocene climate variability
899 in the South Adriatic Sea. Clim. Past 9, 499–515. https://doi.org/10.5194/cp-9-499-2013
900 Siani, G., Paterne, M., Colin, C., 2010. Late glacial to Holocene planktic foraminifera bioevents and climatic record in the South
901 Adriatic Sea. J. Quat. Sci. 25, 808–821. https://doi.org/10.1002/jqs.1360
902 Siani, G., Sulpizio, R., Paterne, M., Sbrana, A., 2004. Tephrostratigraphy study for the last 18,000 14C years in a deep-sea sediment
903 sequence for the South Adriatic. Quat. Sci. Rev. 23, 2485–2500. https://doi.org/10.1016/j.quascirev.2004.06.004
904 Sicre, M.-A., Peltzer, E.T., 2004. Lipid geochemistry of remote aerosols from the southwestern Pacific Ocean sector. Atmos.
905 Environ. 38, 1615–1624. https://doi.org/10.1016/j.atmosenv.2003.12.012
906 Sicre, M.-A., Siani, G., Genty, D., Kallel, N., Essallami, L., 2013. Seemingly divergent sea surface temperature proxy records in the
907 central Mediterranean during the last deglaciation. Clim. Past 9, 1375–1383. https://doi.org/10.5194/cp-9-1375-2013
908 Sierro, F.J., Hodell, D.A., Andersen, N., Azibeiro, L.A., Jimenez-Espejo, F.J., Bahr, A., Flores, J.A., Ausin, B., Rogerson, M.,
909 Lozano-Luz, R., Lebreiro, S.M., Hernandez-Molina, F.J., 2020. Mediterranean Overflow Over the Last 250 kyr: Freshwater
910 Forcing From the Tropics to the Ice Sheets. Paleoceanogr. Paleoclimatology 35. https://doi.org/10.1029/2020PA003931
911 Sierro, F.J., Hodell, D.A., Curtis, J.H., Flores, J.A., Reguera, I., Colmenero-Hidalgo, E., Bárcena, M.Á.A., Grimalt, J.O., Cacho, I.,
912 Frigola, J., Canals, M., 2005. Impact of iceberg melting on Mediterranean thermohaline circulation during Heinrich events.
913 Paleoceanography 20, 1–13. https://doi.org/10.1029/2004PA001051
914 Sprovieri, R., Di Stefano, E., Incarbona, A., Gargano, M.E., 2003. A high-resolution record of the last deglaciation in the Sicily
915 Channel based on foraminifera and calcareous nannofossil quantitative distribution. Palaeogeogr. Palaeoclimatol. Palaeoecol.
916 202, 119–142. https://doi.org/10.1016/S0031-0182(03)00632-1
917 Stanford, J.D., Rohling, E.J., Bacon, S., Roberts, A.P., Grousset, F.E., Bolshaw, M., 2011. A new concept for the paleoceanographic
918 evolution of Heinrich event 1 in the North Atlantic. Quat. Sci. Rev. 30, 1047–1066.
919 https://doi.org/10.1016/j.quascirev.2011.02.003
920 Stanford, J.D., Rohling, E.J., Hunter, S.E., Roberts, A.P., Rasmussen, S.O., Bard, E., McManus, J., Fairbanks, R.G., 2006. Timing of
921 meltwater pulse 1a and climate responses to meltwater injections. Paleoceanography 21, 1–9.
922 https://doi.org/10.1029/2006PA001340
923 Storms, J.E.A., Weltje, G.J., Terra, G.J., Cattaneo, A., Trincardi, F., 2008. Coastal dynamics under conditions of rapid sea-level rise:
924 Late Pleistocene to Early Holocene evolution of barrier-lagoon systems on the northern Adriatic shelf (Italy). Quat. Sci. Rev.
925 27, 1107–1123. https://doi.org/10.1016/j.quascirev.2008.02.009
926 Ternois, Y., Sicre, M.-A., Paterne, M., 2000. Climatic changes along the northwestern African continental margin over the last 30
927 kyrs. Geophys. Res. Lett. 27, 133–136. https://doi.org/10.1029/1999GL002306
928 Thiede, J., Nees, S., Schulz, H., De Deckker, P., 1997. Oceanic surface conditions recorded on the sea floor of the Southwest Pacific
929 Ocean through the distribution of foraminifers and biogenic silica. Palaeogeogr. Palaeoclimatol. Palaeoecol. 131, 207–239.
930 https://doi.org/10.1016/S0031-0182(97)00004-7
931 Totaro, F., Insinga, D.D., Lirer, F., Margaritelli, G., Caparrós, A.C. i., de la Fuente, M., Petrosino, P., 2022. The Late Pleistocene to
932 Holocene tephra record of ND14Q site (southern Adriatic Sea): Traceability and preservation of Neapolitan explosive products
933 in the marine realm. J. Volcanol. Geotherm. Res. 423, 107461. https://doi.org/10.1016/j.jvolgeores.2021.107461
934 Toucanne, S., Soulet, G., Freslon, N., Silva Jacinto, R., Dennielou, B., Zaragosi, S., Eynaud, F., Bourillet, J.F., Bayon, G., 2015.
935 Millennial-scale fluctuations of the European Ice Sheet at the end of the last glacial, and their potential impact on global
936 climate. Quat. Sci. Rev. 123, 113–133. https://doi.org/10.1016/j.quascirev.2015.06.010

Trigo, R.M., Pozo-Vázquez, D., Osborn, T.J., Castro-Díez, Y., Gámiz-Fortis, S., Esteban-Parra, M.J., 2004. North Atlantic oscillation influence on precipitation, river flow and water resources in the Iberian Peninsula. Int. J. Climatol. 24, 925–944. https://doi.org/10.1002/joc.1048

Trincardi, F., Foglini, F., Verdicchio, G., Asioli, A., Correggiari, A., Minisini, D., Piva, A., Remia, A., Ridente, D., Taviani, M., 2007. The impact of cascading currents on the Bari Canyon System, SW-Adriatic Margin (Central Mediterranean). Mar. Geol. 246, 208–230. https://doi.org/10.1016/j.margeo.2007.01.013

Turchetto, M., Boldrin, A., Langone, L., Miserocchi, S., Tesi, T., Foglini, F., 2007. Particle transport in the Bari Canyon (southern Adriatic Sea). Mar. Geol. 246, 231–247. https://doi.org/10.1016/j.margeo.2007.02.007

Vai, G.B., Cantelli, L., 2004. Litho-paleoenvironmental maps of Italy during the last two climatic extremes.

Voelker, A.H.L., De Abreu, L., Schönfeld, J., Erlenkeuser, H., Abrantes, F., 2009. Hydrographic conditions along the western Iberian margin during marine isotope stage 2. Geochemistry, Geophys. Geosystems 10. https://doi.org/10.1029/2009GC002605

Weltje, G.J., Tjallingii, R., 2008. Calibration of XRF core scanners for quantitative geochemical logging of sediment cores: Theory and application. Earth Planet. Sci. Lett. 274, 423–438. https://doi.org/10.1016/J.EPSL.2008.07.054

Winter, A., Siesser, W.G., 1994. Coccolithophores. Cambridge University Press.

Wirth, S.B., Glur, L., Gilli, A., Anselmetti, F.S., 2013. Holocene flood frequency across the Central Alps - solar forcing and evidence for variations in North Atlantic atmospheric circulation. Quat. Sci. Rev. 80, 112–128. https://doi.org/10.1016/j.quascirev.2013.09.002

Young, J.R., Geisen, M., Cros, L., Kleijne, A., Sprengel, C., Probert, I., Østergaard, J., 2003. A guide to extant coccolithophore taxonomy . J. Nannoplankt. Res. 1, 125.

Zhang, W., Wu, J., Wang, Yi, Wang, Yongjin, Cheng, H., Kong, X., Duan, F., 2014. A detailed East Asian monsoon history surrounding the “Mystery Interval” derived from three Chinese speleothem records. Quat. Res. 82, 154–163. https://doi.org/10.1016/j.yqres.2014.01.010

Figure

Click here to access/download;Figure;Fig 1.jpg

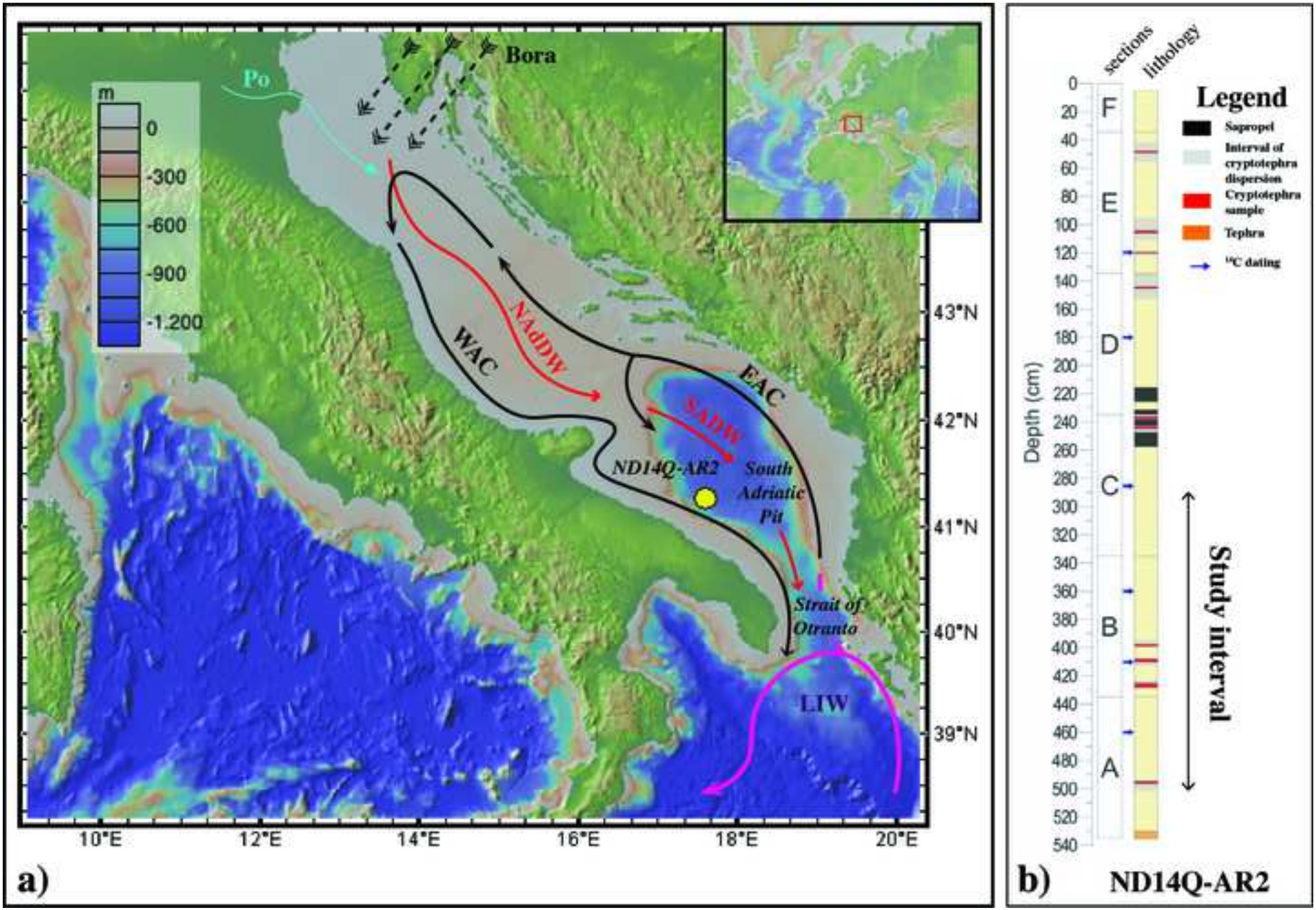

Figure

Click here to access/download;Figure;Fig 2.jpg

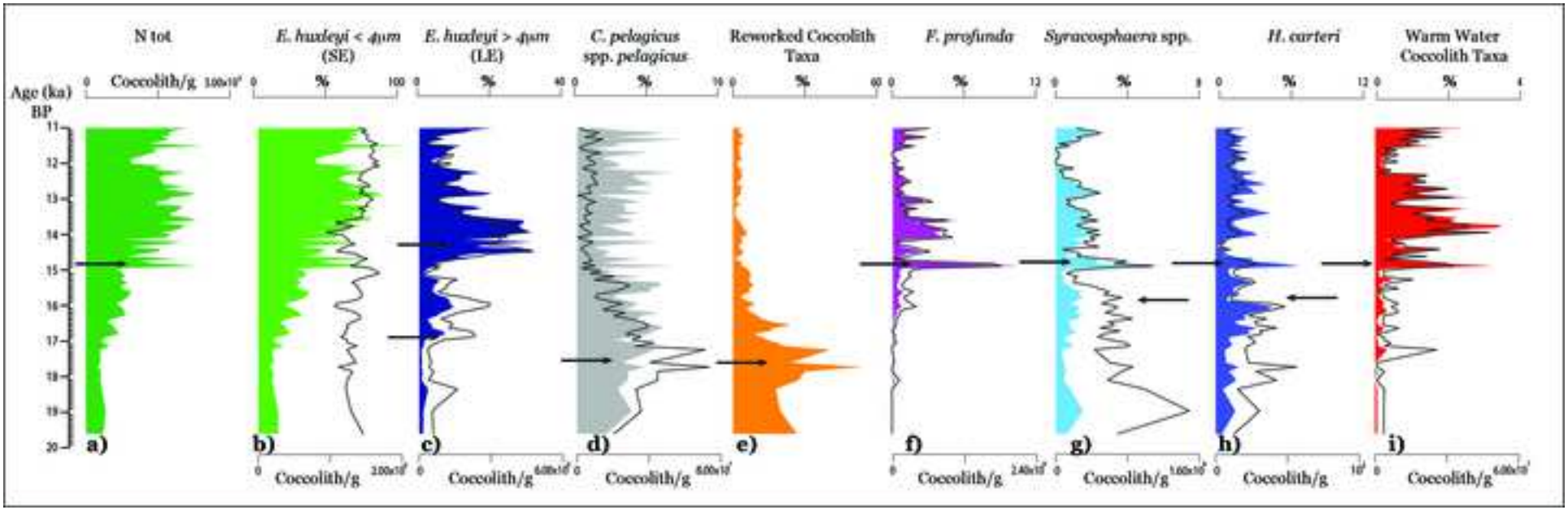

Figure

Click here to access/download;Figure;Fig 3.jpg

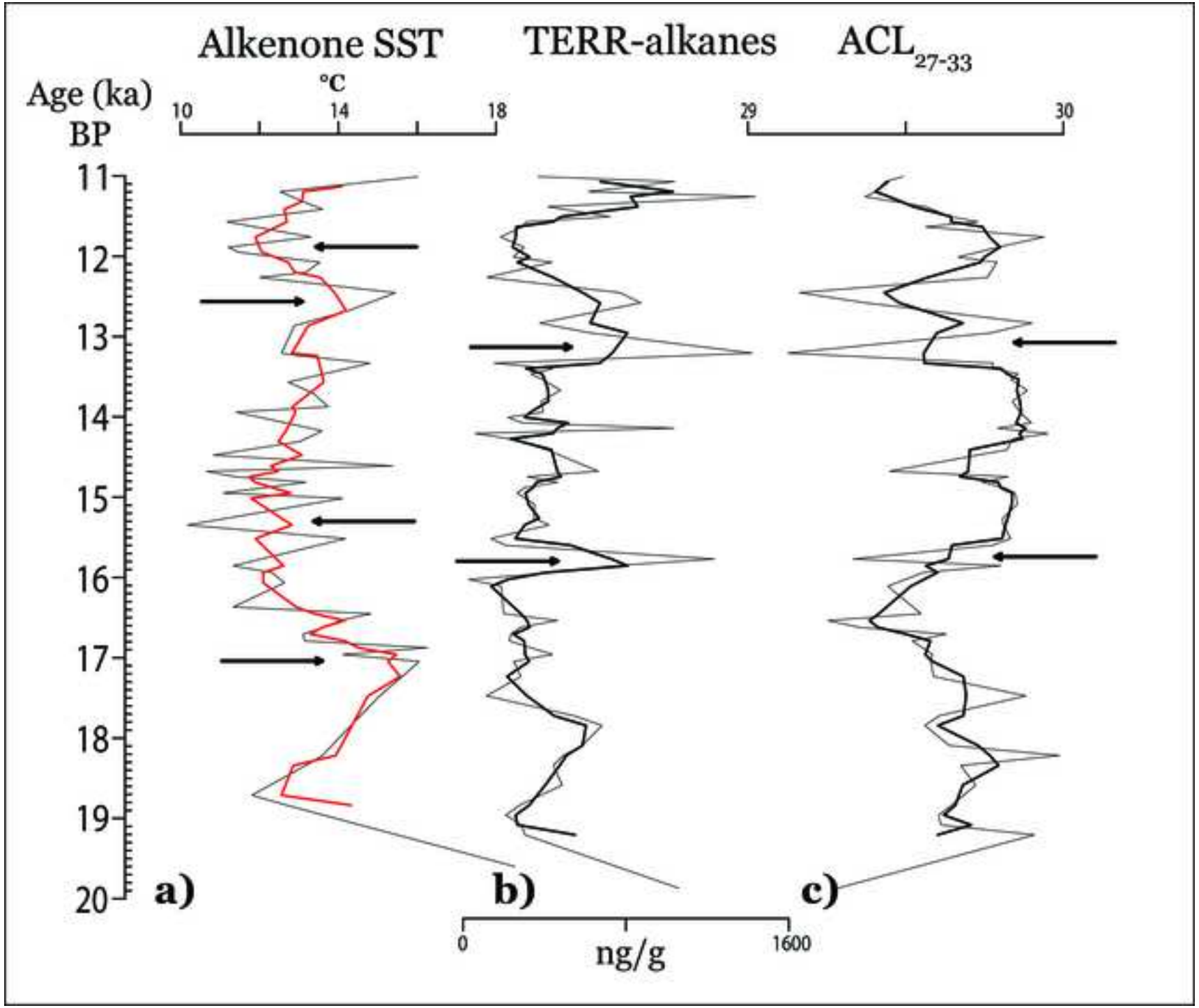

Figure

Click here to access/download;Figure;Fig 4.jpg

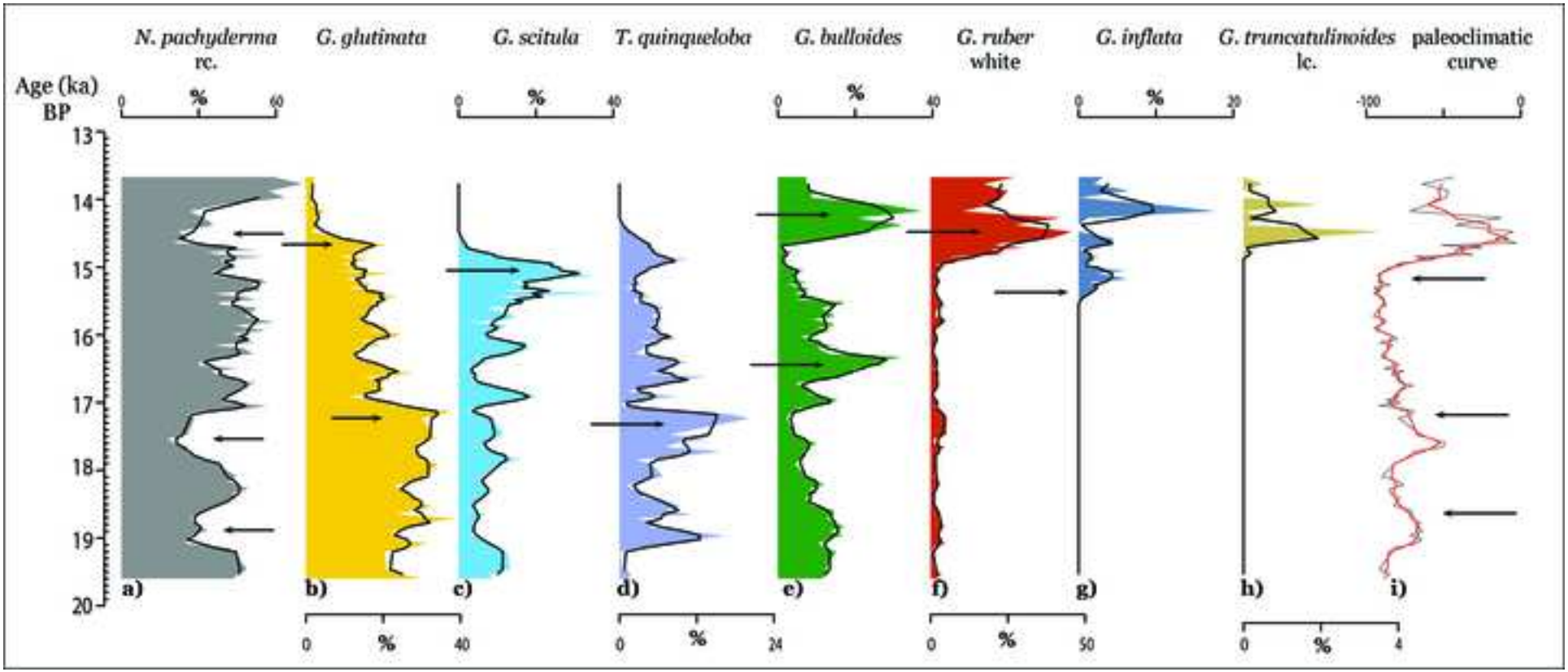

Figure

Click here to access/download;Figure;Fig 5.jpg

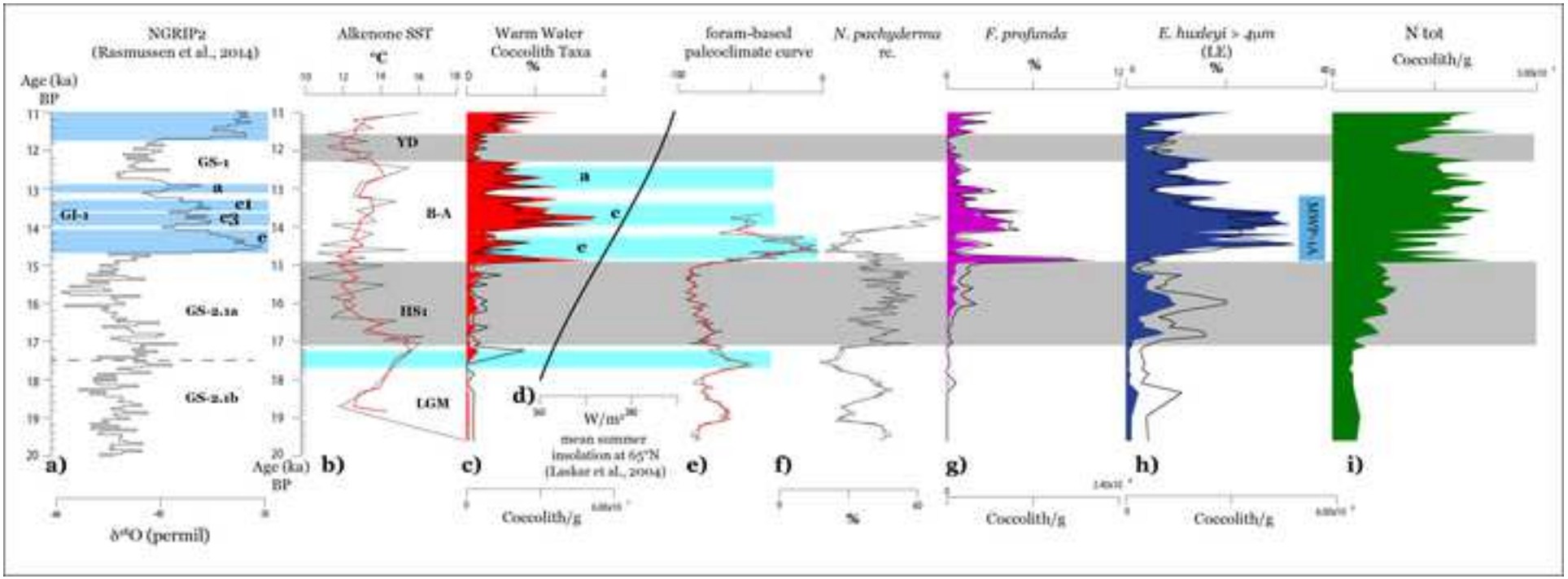

Figure

Click here to access/download;Figure;Fig 6.jpg

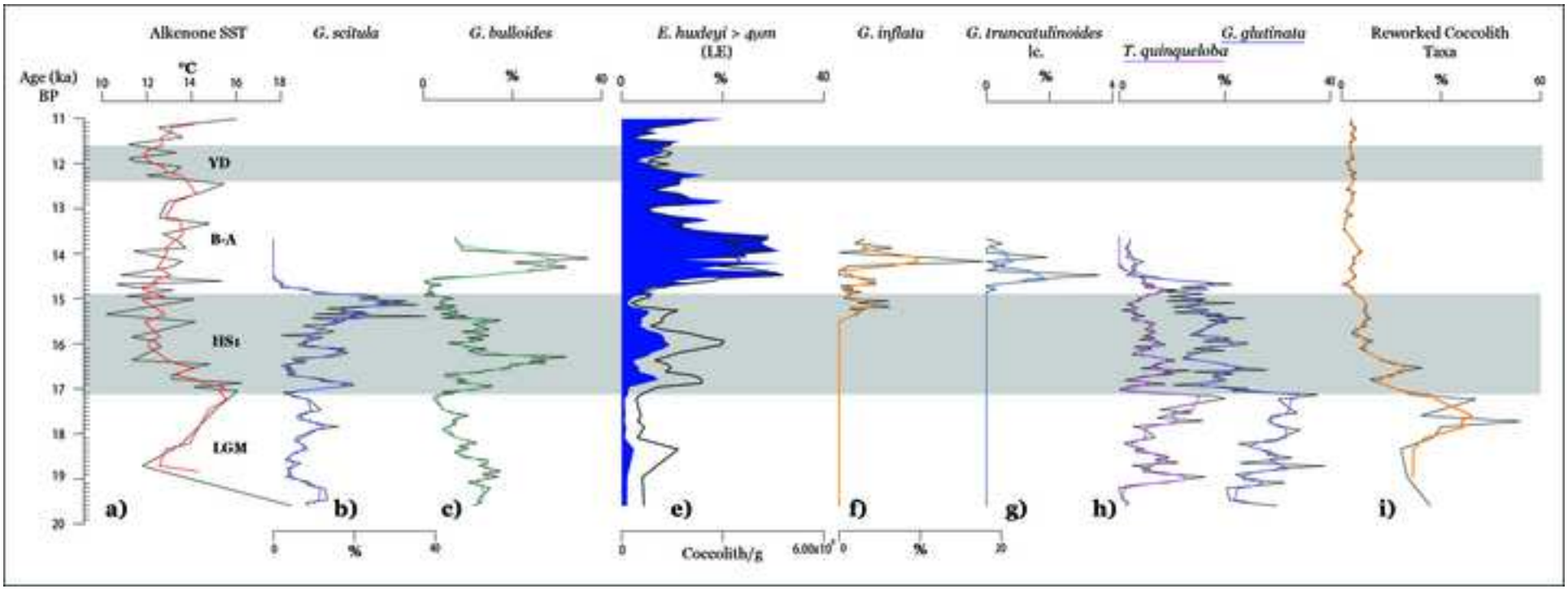

Figure

Click here to access/download;Figure;Fig 7.jpg

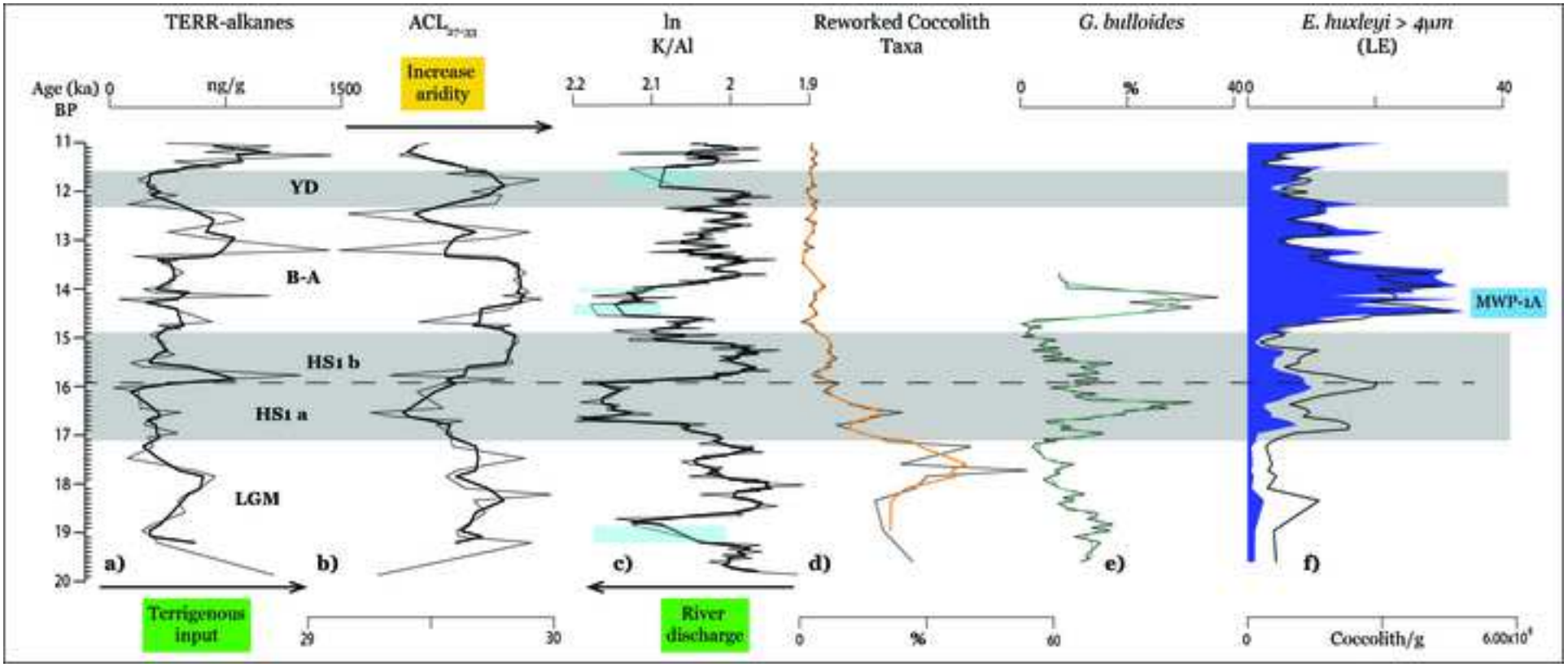

Figure

Click here to access/download;Figure;Fig 8.jpg

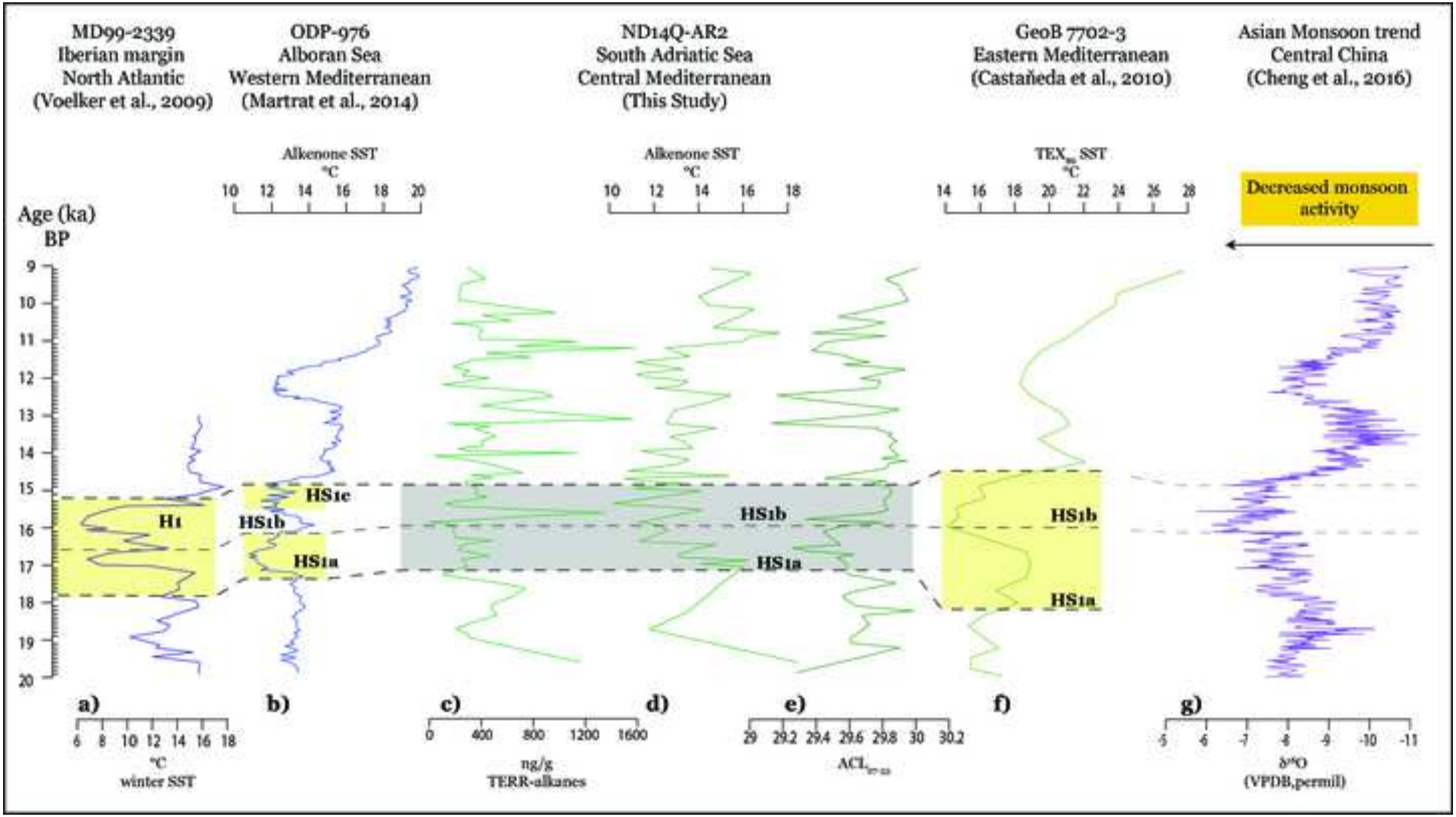

Declaration of interests

☒The authors declare that they have no known competing financial interests or personal relationships that could have appeared to influence the work reported in this paper.

☐The authors declare the following financial interests/personal relationships which may be considered as potential competing interests: